HYBRID MEMBRANES FOR LIGHT GAS SEPARATIONS

A Thesis

by

TING LIU

Submitted to the Office of Graduate Studies of
Texas A&M University
in partial fulfillment of the requirements for the degree of

MASTER OF SCIENCE

May 2012

Major Subject: Chemical Engineering

HYBRID MEMBRANES FOR LIGHT GAS SEPARATIONS

A Thesis

by

TING LIU

Submitted to the Office of Graduate Studies of
Texas A&M University
in partial fulfillment of the requirements for the degree of

MASTER OF SCIENCE

Approved by:

Chair of Committee,	Daniel F. Shantz
Committee Members,	Hae-Kwon Jeong
	Tahir Cagin
	Karen L.Wooley
Head of Department,	Charles Glover

May 2012

Major Subject: Chemical Engineering

ABSTRACT

Hybrid Membranes for Light Gas Separations. (May 2012)

Ting Liu, B.S., Zhejiang University

Chair of Advisory Committee: Dr. Daniel F. Shantz

Membrane separations provide a potentially attractive technology over conventional processes due to their advantages, such as low capital cost and energy consumption. The goal of this thesis is to design hybrid membranes that facilitate specific gas separations, especially olefin/paraffin separations. This thesis focuses on the designing dendrimer-based hybrid membranes on mesoporous alumina for reverse-selective separations, synthesizing Cu(I)-dendrimer hybrid membrane to facilitate olefin/paraffin separations, particularly ethylene/methane separation, and investigating the influence of solvent, stabilizing ligands on facilitated transport membrane.

Reverse-selective gas separations have attracted considerable attention in removing the heavier/larger molecules from gas mixtures. In this study, dendrimer-based chemistry was proved to be an effective method by altering dendrimer structures and

generations. G6-PIP, G4-AMP and G3-XDA are capable to fill the alumina mesopores and slight selectivity are observed.

Facilitated transport membranes were made to increase the olefin/paraffin selectivity based on their chemical interaction with olefin molecules. Two approaches were explored, the first was to combine facilitator Cu(I) with dendrimer hybrid membrane to increase olefin permeance and olefin/paraffin selectivity simultaneously, and second was to facilitate transport membrane functionality by altering solvents and stabilizing ligands. Promising results were found by these two approaches, which were: 1) olefin/paraffin selectivity slightly increased by introducing facilitator Cu(I), 2) the interaction between Cu(I) and dendrimer functional groups are better known.

ACKNOWLEDGEMENTS

First of all, I would like to thank Dr. Daniel F. Shantz for his support and guidance over the past two years that I have been a graduate student in his group. He has been a great teacher and mentor.

I also thank my committee members: Dr. Hae-Kwon Jeong, Dr. Tahir Cagin, Dr. Carl Laird and Dr. Karen L. Wooley for their time, effort and faith they have placed in me.

Thank also go to my friends and labmates, Nataly, Fred, Ben, Ale, Xiang, Qingqing, John and Miyuki. I specially thank Dr. Benjamin Hamilton for his guidance, valuable advice and help on my research and work. It has been a great time to work with them.

My last acknowledgement is saved for my family. Especially, I would like to express my deepest appreciation to my father and mother for their infinite love and support for me.

TABLE OF CONTENTS

Page

ABSTRACT iii

ACKNOWLEDGEMENTS v

TABLE OF CONTENTS vi

LIST OF FIGURES ix

LIST OF TABLES xii

CHAPTER

I INTRODUCTION 1

1.1 Membrane-based gas separations 1
1.2 Membrane categories 3
1.2.1 Hybrid membrane 6
1.2.2 Melamine-based dendrimer hybrid membrane 8
1.3 Olefin/paraffin separations 10
1.4 Gas transport mechanism 13
1.4.1 Gas transport mechanism of porous membrane 14
1.4.2 Solution-diffusion model of polymeric membrane 17
1.4.3 Reverse-selective separations 19
1.4.4 Reversible complexation of olefin/paraffin separations . 19
1.5 Conclusions 21

II EXPERIMENTAL METHODS 22

2.1 Membrane synthesis 22
2.1.1 Materials 22
2.1.2 Dendrimer functionalization of membrane 25

CHAPTER Page

2.1.3 Dendrimer architecture 28
2.2 Synthesis of Cu(I)-dendrimer hybrid membrane 28
2.2.1 Materials 29
2.2.2 Preparation of Cu(I)-dendrimer membrane 29
2.2.3 Cu(I) wet impregnation (RCA treated membrane) 30
2.3 Single gas permeation test 31

III REVERSE SELECTIVE MEMBRANES FORMED BY DENDRIMERS ON MESOPOROUS CERAMIC SUPPORTS 34

3.1 Introduction 34
3.2 Experiment 34
3.3 Results 35
3.3.1 RCA treated membrane 35
3.3.2 Membrane with PIP dendrons 37
3.3.3 Membrane with XDA dendrons 43
3.3.4 Membrane with Allylamine dendrons 48
3.3.5 Membrane with AMP dendrons 49
3.4 Conclusions 53

IV Cu(I)-BASED FACILITATED MEMBRANES FOR OLEFIN/PARAFFIN SEPARATIONS 54

4.1 Introduction 54
4.2 Experiment 55
4.3 Results 56
4.3.1 Cu(I)-AMP dendrimer hybrid membrane 56
4.3.2 Cu(I)-wet impregnation of RCA treated membrane 61
4.3.3 Cu(I)-stabilizing ligand-solvent systems 64
4.4 Conclusions 68

V FUTURE WORK AND CONCLUSIONS 69

5.1 Synthesis of uniform mesoporous silica Membralox® 69
5.2 ATRP-based hybrid membrane 71
5.3 Cu(I)/propionitrile system 72

CHAPTER Page

REFERENCES 73

VITA 80

LIST OF FIGURES

FIGURE Page

1 Relationship between hydrogen permeability and H_2/N_2 selectivity for rubbery (O) and glassy (●) polymers and the empirical upper bound correlation……5

2 Melamine-based G3-PIP dendrimer structure (a), Differential reactivity of triazines (b) ……9

3 Facilitated transport membrane (FTM)……11

4 The contribution of Poiseuille flow and Knudson flow to total flow as a function of the ratio of the pore radius to the mean free path of gas molecules……16

5 Illustration of Cu(I)-olefin complexation interaction……...20

6 SEM image of a cross-section 5nm alumina membrane……..24

7 Synthetic protocols for dendrimer-based membrane…….....26

8 G1- (a), G2- (b) and G3- (c) dendrons……..27

9 General experimental scheme of Cu(I)-dendrons …….……...30

10 Schematic of custom-built permeance measurement gas-rig……...32

11 He permeance as a function of pressure for RCA treated membrane……..35

FIGURE Page

12 He/N_2 selectivity as a function of pressure of RCA treated membrane……...36

13 Permeances for G1-PIP to G7-PIP (G6-PIP and G7-PIP @ 80 psi)……38

14 He permeance of G5-PIP, G6-PIP, G7-PIP and RCA treated membrane…… 39

15 CH_8/He selectivity for each generation (a), Robeson's He/N_2 correlation of separation factor versus permeability for polymeric membrane (b), He/N_2 correlation from G1-PIP to G7-PIP (c)……..... 41

16 Selectivity for PIP-based dendrimer membrane…….. 43

17 Selectivity as a function of permeance for RCA membrane (a) G2-XDA at 5.50 bar (b) and G3-XDA at 5.50 bar (b)…….44

18 Selectivity as a function of permeance for G3-pABA membrane……..……..45

19 G3-XDA and G4-XDA permeance as a function of pressure……..47

20 Selectivity as a function of permeance for G3-Allylamine……..48

21 Permeances comparison between G3-AMP and G4-AMP membranes….....49

22 Selectivity versus permeance for G3-AMP (a) and G4-AMP (b)……50

23 Chemical structure of chelating groups, diethylamine (a), diethylenetriamine (b), propionitrile (c), propylamine (d)……...55

FIGURE Page

24 Selectivity versus permeance for G3-AMP-Cu(I) #1(a), Cu(I)-AMP-Cu(I) #2 (b)…….57

25 Selectivity versus permeance for G4-AMP-Cu(I) membrane……..60

26 Multiple Cu(I)-impregnation synthetic protocols…….62

27 C_3H_6/C_3H_8, C_2H_4/CH_4 selectivity, from left to right represent ideal selectivity, RCA treated membranes, one-, two-, three- and four-time coating with Cu(I), respectively…….63

28 Propylene permeance change as a function of Cu(I) impregnation cycle (a) C_3H_6/C_3H_8 selectivity change as a function of Cu(I) impregnation cycle (b)……..64

29 Permeances for RCA treated membrane before and after Cu(I)/diethylamine/methanol treatment……...65

30 Reduction of N_2 permeance after Cu(I) added into various systems…….....67

31 Selectivity for Cu(I)-propionitrile membrane (120˚C)…….67

32 Synthesis methods for defect-free membrane: (a) simple dip-coating, and (b) inside dip-coating…….70

33 Synthetic protocols for ATRP functionalized mesoporous alumina membrane…….72

LIST OF TABLES

TABLE Page

1 The relationship between physical/chemical property and separation process….....3

2 Ideal selectivity (Knudson diffusion)…….....17

3 Different linking groups and capping groups……...28

4 The effect of dendrimer generation on permeance..……..…...52

CHAPTER I

INTRODUCTION

1.1 Membrane-based Gas Separations

Membrane-based separations provide a potential alternative technology for a large number of industrial applications in the pharmaceutical, biotechnology and chemical industries. In general terms, membrane separations can be described by a feed stream that passes through the membrane, and that the remaining feed is rejected, remained or concentrated [1]. This technology delivers many benefits such as continuous operation, low energy consumption, capital and operating costs [2].

Over the past few decades, a number of membrane processes have been commercialized and some new types of membranes are still undergoing development. The first commercial membrane was manufactured based on the early work of Zsigmondy after 1914 [3]. Then the work done by Henis and Tripodi [4] made industrial gas separation economically feasible. The first microfiltration and ultrafiltration

---

This thesis follows the style of Journal of Membrane Science.

membrane was studied by Ferry in 1930 [5]. A breakthrough in the application of industrial membranes was the development of asymmetric membranes in Loeb and Sourirajan's lab [6]. This membrane typically consists of a very thin top layer and a porous sub layer as the support.

Intrinsic physical/chemical properties such as size, vapor pressure, freezing point, affinity, charge, density and chemical nature of the components to be separated suggest corresponding membrane types [2]. Researchers have also performed numerous studies on finding promising membrane materials including hybrid membranes, facilitated transport membranes, etc [7]. Table 1 shows the separation processes and the corresponding physical/chemical property utilized to achieve separation. Gas separations are potential large-scale applications for membranes. It is envisioned that membranes could achieve comparable separations over more energy-intensive processes, e.g. cryogenic, distillation [8].

Table 1. The relationship between physical/chemical property and separation process [2]

Physical/chemical property	**Separation process**
Size	Filtration, microfiltration, ultrafiltration, dialysis, **gas separation**
Vapor pressure	Distillation, membrane distillation
Freezing point	Extraction, absorption, reverse osmosis
Affinity	**Gas separation**, pervaporation, affinity chromatography
Charge	Ion exchange, electrodialysis, electrophoresis, diffusion dialysis
Density	Centrifugation
Chemical nature	Complexation, carrier mediated transport

1.2 Membrane Categories

Membranes fall into two material categories: organic and inorganic membranes. Inorganic membranes have attracted considerable attention due to their thermal/chemical stability, while polymeric membranes cannot function above 500 ^{0}C [9]. Ceramic, glass, metallic and zeolite membranes are the major types of inorganic membranes. Among these types, ceramic membranes have pore sizes between 0.05-20 μm, and are usually fabricated from inorganic materials (such as silicon carbide and zirconium oxide). The protocols involved are mainly sol-gel methods and calcinations that can be adjusted to yield the desired oxide form and pore size [10]. These membranes are widely used in micro and ultrafiltration processes [11]. Zeolite membranes have a crystalline network of SiO_4 and AlO_4. This tetrahedral structure provides a large number of cations, which

determines the pore size of zeolite membrane. However, the large-scale manufacturing of zeolites membranes is challenging since they are brittle [1,2].

Generally organic membranes are typically referred to as synthetic or natural polymeric membranes. Polymers are attractive materials because they possess a wide range of physical and mechanical properties, such as chain flexibility and high surface area. Fabricating polymers into various shapes will result in different membrane types, which are not available to inorganic materials. Robeson discovered a tradeoff relationship between selectivity and permeability for polymeric membranes (Figure 1)[12]. Namely, polymeric membranes that allow more gas to go through, i.e. membranes with high permeance are usually less selective. However, polymeric membranes with high permeability and selectivity are desirable. As less membrane surface is needed to treat a given amount of gas, this would in turn decrease the capital cost of the membranes [13]. This presence of a tradeoff relationship strongly suggests the limitation of polymeric membranes.

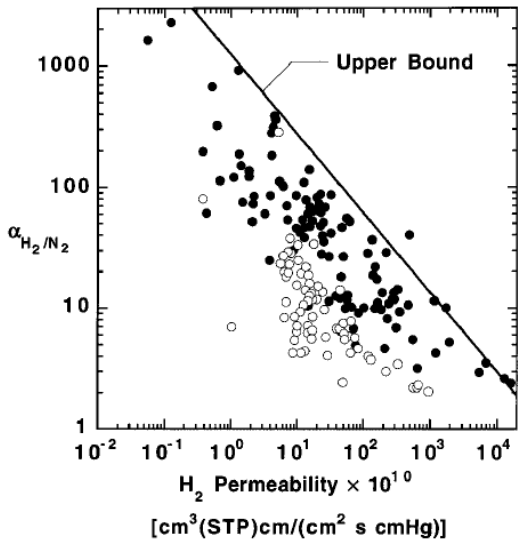

Figure 1. Relationship between hydrogen permeability and H_2/N_2 selectivity for rubbery (O) and glassy (●) polymers and the empirical upper bound correlation [12].

A few examples of fabricating a variety of polymeric membranes have been studied in the past. By far the most common technically used membranes are made by phase separation method. Generally this method includes four steps: 1) precipitation in a non-solvent; 2) solvent evaporation; 3) precipitation by absorption of non-solvent from the vapor phase; 4) precipitation by cooling [14].

Another classification is porous membranes and nonporous membranes. Porous membranes have a well-defined pore size, in the range of 0.1 – 10 μm for microfiltration and 2 – 100 nm for ultrafiltration, respectively. Selectivity is primarily determined by the variation of pore size, but the properties of materials also affect adsorption and chemical

stability. Several techniques are employed to prepare microfiltration membranes, such as sinterting, stretching, and track-etching. However, these are not commonly used for ultrafiltration membranes. Most ultrafiltration membranes are prepared by phase inversion, due to their relatively smaller pore size compared to microfiltration membranes [15].

The separation performance of porous membranes is defined by the diffusivity difference of the gases, which is an acceptable metric for separating gas pairs with similar chemical properties but different molecular sizes. When the sizes of molecules are very similar, porous membranes cannot usually effectively separate the mixtures [16].

1.2.1 Hybrid Membrane

The separation factors and physical properties of inorganic and organic membranes limit their applicability. The next generation of materials, called 'hybrid' membranes, is designed to bridge the gaps between inorganic and organic membranes [17]. Hybrid membranes achieved separations are simultaneously delivering specific chemistry and free volume for a certain application.

Okui and Saitio's lab made the first hybrid membrane from phenyltrimethoxysilane (PTMOS) and tetramethoxysilane (TMOS). These hybrid

membranes were fabricated on a α-alumina porous support and then thermally treated into a certain degree of conversion from gel to glass. The permeation results showed an improvement for both permeability and selectivity [18]. The concept of 'surface-derivatization' has been used to make hybrid membranes. Miller and Koros [19] tried to attach trichlorosilane oligomers to mesoporous alumina membranes with an average pore size of 40 Å. In this way, the pores were effectively filled with aliphatic oligomers, straight, needle-like structures. More recently, Paterson and co-worker performed similar modifications to ceramic membranes using wet chemistry [20]. Similarly, McCarley and Way modified a 5-nm alumina membrane with C18 trichlorosilane [21]. This type of membrane exhibited significant selectivity increasing of heavier/lighter gas pairs. Ford functionalized porous (5-10 nm) alumina membrane with alkyl trichlorosilanes having chain length from C1 to C28. The membrane clearly showed the relationship between pore size and chain length, and the selectivity for heavier organic species become greater. Ford and Javaid also investigated octadecytrichlorosilane (OTS) and phenyltrichlorosilane (PTS) modified porous alumina membranes on the toluene/nitrogen separations [22]. Polymeric membranes filled with nanoparticles attract tremendous attention for application such as optics and catalysis. Merkel and Freeman discovered high permeability and selectivity for large/heavy molecules by introducing

nanoscale fumed silica particles into glassy amorphous poly(4-methyl-2-pentyne) polymers, which surprisingly showed high permeability for hydrocarbon gases [23].

1.2.2 Melamine-based Dendrimer Hybrid Membrane

Subsequent work has investigated more complex organic motifs on ceramic membrane. Our lab [24-27] in collaboration with others has introduced melamine-based dendrimers onto membranes. Dendrimer-functionalized membranes are highly tunable due to their hyperbranched structures and chemical diversities [28]. A melamine-based dendrimer consists of, at minimum, two parts: a cyanuramide or triaminotriazine core and diamine branches [29]. The chemistry developed in Simanek's lab mainly focused on secondary amines. Figure 2 (a) shows the structure of a G3-PIP dendron. Here, cyanuric chloride provides the core and piperazine is the diamine linker [30]. The differential reactivity of triazines can be used to control the chemical reactions between triazine rings and diamine linker groups. Melamine-based dendrimers are potential filling agents for hybrid membranes. The dendrimer size can be manipulated by changing dendrimer generation, and is straightforward given the iterative synthesis process. These groups could possibly deliver high permeability and selectivity due to their high free volume and tailorable chemistry. Figure 2 (b) describes chemoselective reactivity of cyanuric chloride. The first substitution occurs at 0 ^{0}C, and the second

substitution at 25 ^{0}C and the third 70^{0}C [31]. The stepwise substitution of triazine efficiently provides surface functional groups for dendrimers.

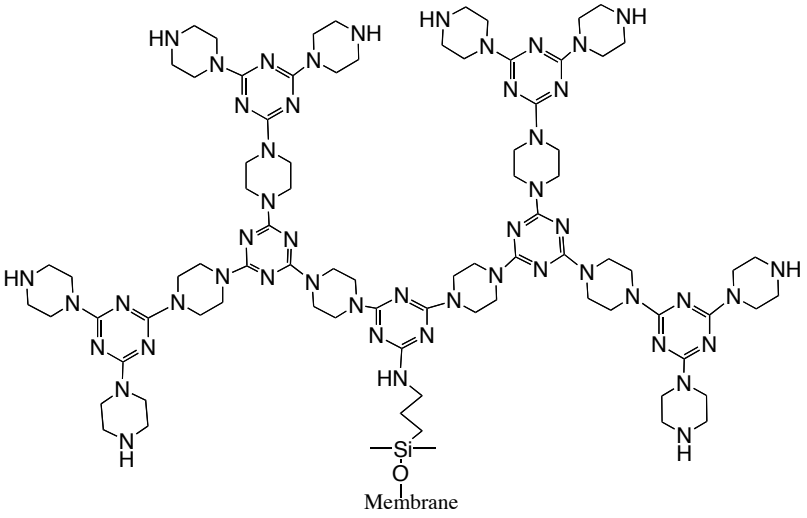

(a)

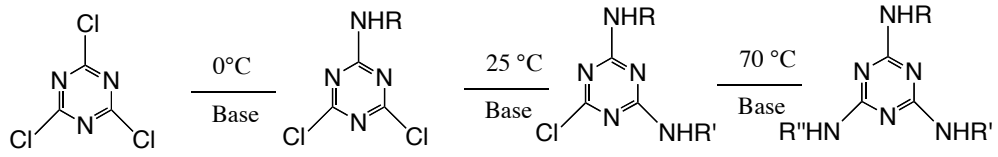

(b)

Figure 2. Melamine-based G3-PIP dendrons (a), differential reactivity of triazines (b) [31].

The technique and applications of synthesizing dendrimers based on melamine have been developed by Simanek's laboratory in 2000. Moreover, a variety of diamine linking groups with varying polarities, hydrophobicites and rigidities have been explored for specific applications [32], ranging from piperazine, 4-aminobenzylamine to p-xylylenediamine. Lim and Simanek [33] achieved an impressive accomplishment, by introducing levulinic/disulphide intermediates to dendrimer chemistry. Moreno and Simanek [34] investigated the drug delivery application after deprotection of the BOC-protected amine and polyethylene glycolylation.

1.3 Olefin/Paraffin Separations

Olefin/paraffin separations are crucial processes in the petroleum industry because low molecule weight olefins such as ethylene (C_2H_4) and propylene (C_3H_8) are important raw materials for polymer product synthesis [35]. Cryogenic distillation has been the dominant technology for olefin/paraffin separations for a long time due to its developed and reliable operations. However, the low temperature and high pressure makes it a highly energy-intensive separation processes since the boiling temperatures are similar. One study reported that 0.12 Quads (1 Quad = 10^{15} BTU) of energy is consumed every year for cryogenic distillation of olefin/paraffin separations [36]. Thus, given the huge economic incentives, innumerable studies have investigated alternate

routes in olefin/paraffin separations. Facilitated transport membranes (FTM) are one of the routes investigated, including immobilized liquid membranes (ILMS) and solvent-swollen, fixed-site carrier membranes. Theoretically it can increase olefin permeability via chemical complexation, in addition to penetrant dissolution and diffusion [37]. Facilitated transport can similarly be viewed as a chemical adsorption process on the feed side of the membrane and a stripping process on the permeate side of the membrane.

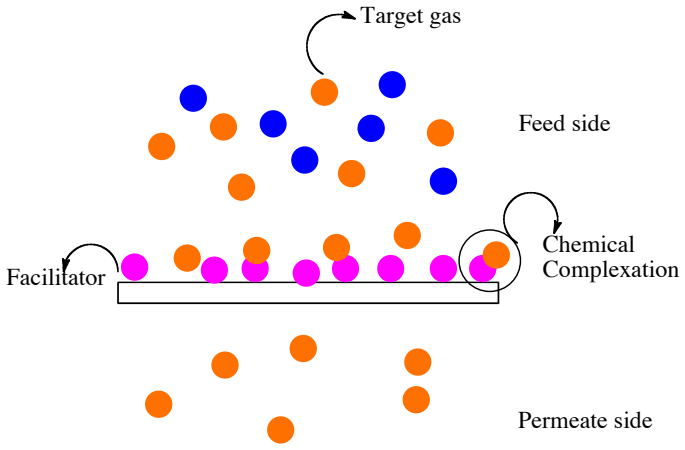

Figure 3. Facilitated transport membrane (FTM).

As is shown in the Figure 3, the chemical complexation reaction creates another transport mechanism in addition to the solution-diffusion mechanism [38]. The overall

transport process can be described as having two parts, the first is gas molecule adsorption on the membrane surface, and second is diffusion based on the concentration gradient or reaction with the complexation agents or carries species. Thus, there are two contributions to the overall transport process: (1) the diffusion of uncomplexed gas molecules and (2) diffusion of carrier-gas complexes. Therefore, the diffusion of carrier-gas complexes improves the selectivity of facilitated transport membranes, which are usually higher than other conventional membrane separations.

Hughes *et* al. [39] described supported liquid membranes of aqueous $AgNO_3$ solution in a porous cellulose acetate membrane for ethylene/ethane separation. Pinnau [40] introduced solid polymer electrolyte, based on rubbery, containing a dissolved olefin-complexing metal salt to overcome the traditional limitation of facilitated transport membranes, such as poor mechanical stability, preparation difficulty and mobility provider.

Reversible reactions can occur between some transition metals and olefins. There is evidence suggesting that Cu(I) exhibits strong affinity capacity with olefins due to its lost electron in the outer shell. Usually the intensity of π-complexation between transition metal ion and olefin is primarily determined by the electronegativity of the metal, which is a measure of the relative strength of an atom to attract bonding electrons. With the greater electronegativity, the metal atom draws electrons more strongly. If the

metal electronegativity is substantially high, the metal is not practical due to its irreversible reaction and vice versa. Cu(I) or Ag(I) are commonly selected as facilitators due to their low cost and suitable electronegativity [41].

Both aqueous and nonaqueous systems of Cu(I)/Ag(I) have been studied. For example, the cupric state of Cu(I) is more stable in the aqueous systems [42], then reactions tend to the occurrence of disproportionation to Cu(II) and copper metal. However, nonaqueous copper solution (CuTFA) also shows less possibility of disproportionation and does not require additional stabilizing agent [43]. In the complexing process, the disproportionation occurrence tendency dramatically effects the function of Cu(I)/Ag(I). In order to improve the stability of facilitated transport membranes, complexation agents can be attached to the polymer chains, dendrimers or other active chelating groups to prevent disproportionation [44].

1.4 Gas Transport Mechanism

When gases pass through a membrane the flux can be expressed by Darcy's law

$$J = -P(\frac{dp}{dx}) \tag{1-1}$$

where J is the flux of gas through the membrane, P is the permeability and dp/dx is the pressure gradient of gas across the membrane. At steady state, when P is constant, Eq.(1-1) can be integrated to

$$J = P\frac{\Delta p}{l} \tag{1-2}$$

where Δp is the transmembrane pressure drop, and l is the thickness of the membrane. Along with the permeability, permeance P (Eqn. 1.3) is used to express the gas transport when the active layer of membrane is not known.

$$\mathrm{P} = \frac{P}{l} = \frac{J}{\Delta p} \tag{1-3}$$

1.4.1 Gas Transport Mechanism of Porous Membrane

Poiseuille flow [45] (viscous flow), Knudsen flow, surface diffusion and capillary condensation [46] are the most common types of flow regimes that occur when gases pass through porous materials. Poiseuille flow or Knudsen flow is usually identified by the relative ratio between pore size and the mean free path of gas molecules. Typically when the pore size is significantly larger than the gas mean free path ($r/\lambda > 5$), Poiseuille flow dominates the transport process. However, when the pore size is much smaller than the gas mean free path ($r/\lambda < 0.5$), Knudsen flow is the

dominant transport mechanism. Usually the dependency of the permeance on pressure can be applied to identify the dominant transport mechanism. The permeability in Poiseuille flow is given by:

$$P_v = \left(\frac{\varepsilon}{t}\right)\frac{r^2 \Delta p}{8\eta RT} \tag{1-4}$$

The permeability in Knudsen flow is expressed as follows:

$$P_k = \frac{2r}{s}\left(\frac{\varepsilon}{t}\right)\sqrt{\frac{8}{\pi MRT}} \tag{1-5}$$

where, ε is the membrane porosity, τ is the pore tortuosity which is assumed to be unity in parallel and uniform capillaries, r is the pore radius, η is the gas viscosity, T is the temperature, M is the molecular weight of the gas, and Δp is transmembrane pressure drop. Figure 4 shows the relative relation between pore size and its respective dominant flow type.

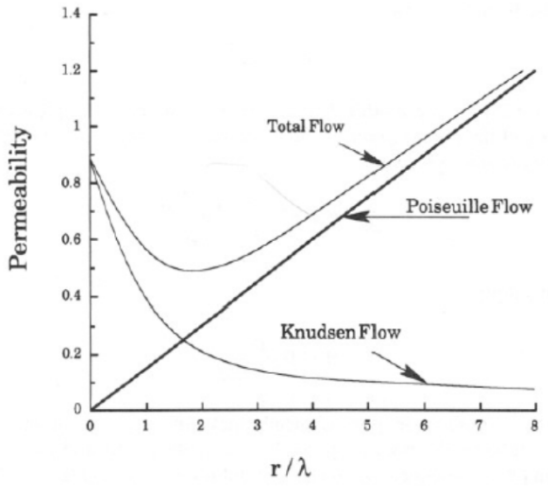

Figure 4. The contribution of Poiseuille flow and Knudson flow to total flow as a function of the ratio of the pore radius to the mean free path of gas molecules [6].

RCA treatment is a standard set of cleaning steps for removing organic contaminants, thin oxide layers and ionic contamination [47]. After RCA treatment, membranes should be contaminant free. Table 2 shows the ideal selectivity if Knudsen transport dominates for several gas pairs. The occurrence of Knudsen flow or Poiseuille flow is greatly dependent on the pore size of the membrane. For the 5 nm Membralox® bare membrane and assuming the defects in the mesoporous layer to be negligible, the $r/\lambda<0.5$ and the flow is in the Knudsen flow region, collisions between the gas and pore wall are more frequent than collisions between gas molecules. If the flow is dominated by Knudsen flow, the permeance is given by Eqn 1-6:

$$P=\frac{2r}{3}(\frac{\varepsilon}{\tau})\sqrt{\frac{8}{\pi MRT}} \quad (1\text{-}6)$$

The permeance is primarily determined by the molecular weight of a gas because other parameters in the equation are decided by physical properties of the membrane, such as porosity, pore size and tortuosity. The He/N_2 selectivity can be calculated to be 2.65. If there are pinhole defects in the membrane substrate, the He/N_2 selectivity will be less than 2.65.

Table 2. Ideal selectivity (Knudson diffusion).

Gas	He/N_2	CO_2/N_2	CO_2/CH_4	C_2H_4/CH_4	C_2H_4/C_2H_6	C_3H_6/C_3H_8	C_3H_8/N_2
Selectivity	2.65	0.80	0.60	0.76	1.04	1.02	0.80

1.4.2 Solution-diffusion Model of Polymeric Membrane

Polymeric and nonporous inorganic membranes are divided into transport categories based on the solution-diffusion mechanism. This model can be derived from Fick's law:

$$J = -D\frac{dc}{dz} \quad (1\text{-}7)$$

where J is the flux, D is the diffusion coefficient, and dc/dz is the concentration gradient of the gas across the membrane. For the equation described above, the permeability is given as:

$$P = \overline{D} \cdot \overline{S} \tag{1-8}$$

where $\overline{D}$ is the average diffusion coefficient and $\overline{S}$ is the average solubility coefficient of the gas. For rubbery polymers, the solubility coefficient is constant and permeability is a strong function of the diffusion coefficient. The permeability is given as:

$$P = DK_D \tag{1-9}$$

where K_D is the Henry's law solubility coefficient. For glassy polymers, the gas solubility is not constant and the permeability can be expressed as the dual-mode sorption model. The permeability in this theory is given as:

$$P = K_D D_D \left(1 + \frac{FK}{1 + bp}\right) \tag{1-10}$$

where D_D is the diffusion coefficient in the Henry's law regime, F is the ratio of diffusion coefficients(Langmuir/Henry), and b is the Langmuir affinity constant.

1.4.3 Reverse-selective Separations

In any type of membrane separation the selectivity of one component (A) over another component (B) is defined as the ratio of permeability, which consists of both diffusivity and solubility given by:

$$\alpha_{A/B} = \frac{P_A}{P_B} = \frac{D_A}{D_B} \times \frac{S_A}{S_B} \quad (1\text{-}11)$$

However, in reverse-selective gas separations (solubility-based gas separations) the larger/heavier molecules preferentially permeate based on their greater solubility as unity ratio of diffusivity, which exhibits positive correlation between selectivity and permeability. This kind of membrane exhibits excellent performance in removing larger/heavier hydrocarbons from small molecules such as hydrogen or natural gas [48].

1.4.4 Reversible Complexation of Olefin/paraffin Separations

The complexation reaction between metal and olefin has been well known. The platinum(II)-ethylene complex known as Zeise's salt was first discovered in 1827 [49]. The comprehensive mechanism was introduced by Dr. Dewar in 1951. The Dewar-Chatt-Duncanson model is the most applicable mechanism for the Cu(I)-olefin complexation reaction [50, 51], explained by Figure 5. This model explains chemical

complexation theory between the π bond of olefins and metal atoms. Both the π bonds of olefin gas and Cu(I) behave as electron donors and electron acceptors. For Cu(I) the outer orbital is empty with one electron lost. A new σ bond is formed due to the overlap of the vacant outermost orbital with the π bond molecular orbital of the olefin, where Cu(I) behaves as an electron acceptor and olefin behaves as an electron donor. Another π bond is formed due to electron donating from the d atomic orbital of the metal to the vacant π* (antibonding) of the olefin, where Cu(I) acts as an electron donor and olefin as an electron acceptor [48].

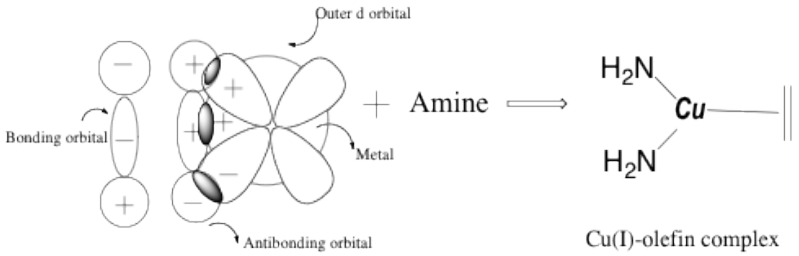

Figure 5. Illustration of Cu(I)-olefin complexation interaction.

Theoretically the other metals in the same family, such as silver and gold, have similar valence characteristic properties as copper. Experimental data shows that bonding strength increase in the order Ag(I) < Cu(I) < Au(I) [52]. Although gold

exhibits better behavior in bonding strength, silver and copper are more practical due to their relatively low cost. Additional stabilizing ligands are added to increase the stability of the Cu(I)-olefin complex, which will prevent the disproportionation of Cu(I) in aqueous solution.

1.5 Conclusions

Solubility-based membrane separations with simultaneous high selectivity and permeability are desired for gas separations. Hybrid membranes combining the advantages for both organic and inorganic membranes could be designed for solubility-based separation. Hybrid membranes based on melamine dendrimers for heavier/lighter gas separations, are explored in the research here. The melamine-based dendrimers are effective filling agents and can be simply tailored to address various sizes.

Facilitated transport membranes with carriers Cu(I)/Ag(I) have been attractive for olefin/paraffin separations, which will substantially increase the solubility of olefins. Also facilitator carrier Cu(I)/Ag(I), attached to dendrimer membrane, have been further discussed in the work here to approach the goal at maximum.

CHAPTER II

EXPERIMENTAL METHODS

In this chapter, general information about the materials and the synthesis procedures for the hybrid membranes are described. More detailed or additional information is given in each chapter.

2.1 Membrane Synthesis

Dendrimer-functionalized hybrid membranes for gas separations were prepared using melamine-based chemistry. This thesis assessed the effects of dendrimer chemistry and size by altering the dendrimer generations, linking groups and capping groups.

2.1.1 Materials

Ethanol, methanol, toluene, dichloromethane (DCM) and tetrahydrofuran (THF) (all ACS reagent grade) were purchased from BDH. Hydrochloric acid (37%, w/w) was purchased from Aldrich. Hydrogen peroxide (30%, w/w) was purchased from BDH. Ammonium hydroxide (28-30%, w/w) was purchased from EMD. 3-

Aminopropyldimethyethoxysilane (APMES, 99%) was purchased from Gelest Inc. Piperazine (>99%), N, N-diisopropylethylamine (DIPEA, purified by redistillation, 99.5%), cyanuric chloride, allylamine, 4-aminobenzylamine (99%), p-xylylenediamine, and 4-aminomethylpiperdine (96%) were purchased from Aldrich. All chemicals were used as received. Water was purified using a Barnstead pure water purification system.

The membranes used in this work were 5nm Membralox®, T1-70-25G, tubular membranes purchased from Pall Co. Florida. This membrane consists of an inner mesoporous γ-alumina layer deposited on the inside of a macroporous α-alumina support tube. The thicknesses of the 5nm mesoporous and 12 nm macroporous layers are 4μm and 3μm, respectively. The original tube length is 25 cm. Figure 6 shows a scanning electron micrograph (SEM) image of the membrane cross section [53].

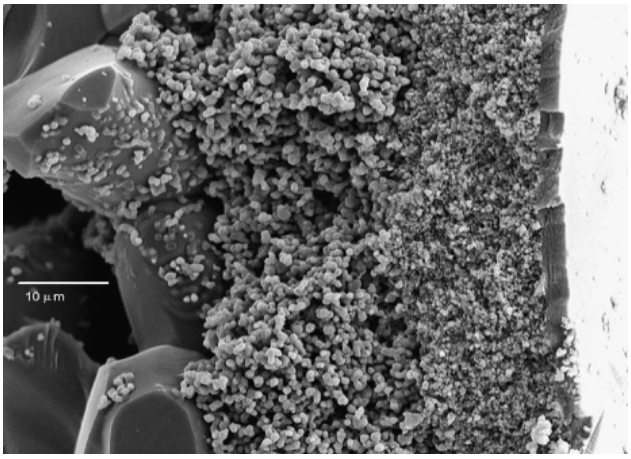

Figure 6. SEM image of a cross-section 5nm alumina membrane [53].

The membrane was cut into 1 in. pieces with a laboratory glasscutter. After cutting, the membranes were cleaned by immersing in a 2:1 ethanol/water solution for 24 h at ambient temperature. Then the membrane was vacuum dried at 100 ˚C for 4 h, and stored in the desiccator until RCA (Radio Corporation of America) treatment. A solution containing 11ml NH_4OH (28%-30%), 11ml H_2O_2 (10%) and 53ml deionized water at ambient temperature was prepared. The membrane was added to this solution in a water bath at 70˚C for 15 min, followed by washing the membrane five times with 100 ml of deionized water and gently rocking each time. Then the acid solution was prepared with 10ml HCl (35%), 10ml H_2O_2 (10%) and 56 ml deionized water. The membrane was added to this solution in water bath at 70 °C for 15 minutes, followed by five washing

with deionized water. After the final deionized water rinsing, the membrane was vacuum dried at 100˚C for 4 h before amine functionalization.

2.1.2 Dendrimer Functionalization of Membrane

Figure 7 shows a scheme with the synthetic protocol used. Amine functionalization was performed by placing a RCA treated membrane into a solution consisting of 0.8 g APDMES (0.1 M), 1ml DIPEA, and 50 ml toluene for 24 h at 70˚C, followed by rinsing 3 times with 20 ml of toluene, and 4 times with 20 ml of THF. These amines were used as a handle from which the dendrimer chemistry is performed. An example is given here where piperazine is used. First, a silane treated membrane was immersed into a solution containing 1.4g cyanuric chloride dissolved in 1ml DIPEA and 50 ml THF for 10h with constant agitation (30 rpm). The membrane was then rinsed 3 times with 20 ml of THF, 2 times with 20 ml of methanol, 2 times with 20 ml of DCM and 2 times with 20 ml of THF. Thin layer chromatography (TLC) was used to check for trace amounts of triazine and amine after final THF rinsing. After forming the dichlorotriazine on the membrane surface, piperazine was reacted with the dichlorotraizine intermediate by dissolving 1.3g piperazine (0.3M) in 50 ml THF at 60 ˚C for 14 h. The treated membrane was rinsed 3 times with 20 ml of THF, 2 times with

20 ml of methanol, 2 times with 20 ml of DCM, and 2 times with 20 ml of THF. Thin layer chromatography (TLC) was used to check for trace amounts of triazine and amine. This procedure leads to the formation of the first generation dendron. This process is repeated to make higher generation dendrons. At the end of the synthesis the membrane was vacuum dried at 100 °C overnight, and then stored in a vial until use. Figure 8 shows G1- through G3-dendrons.

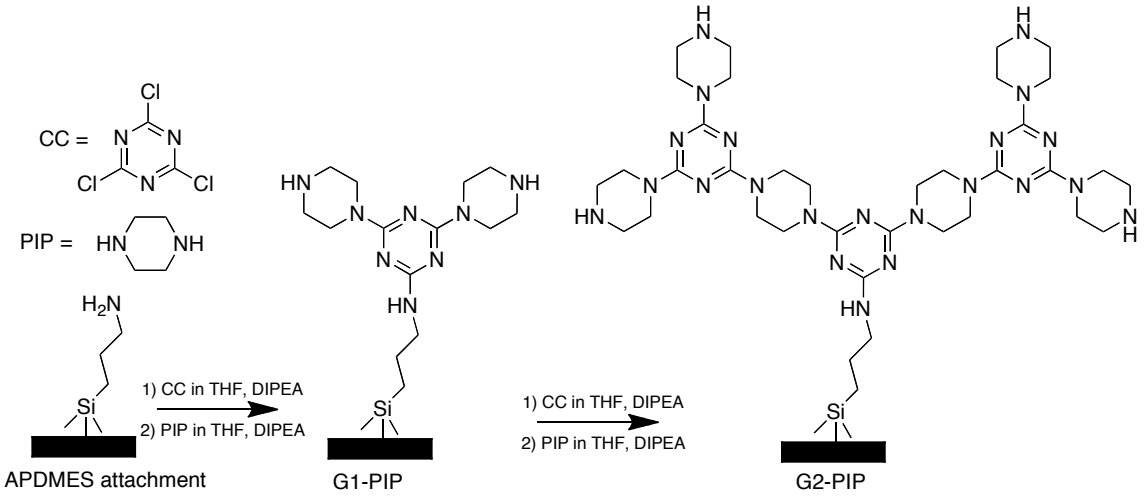

Figure 7. Synthetic protocols for dendrimer-based membrane.

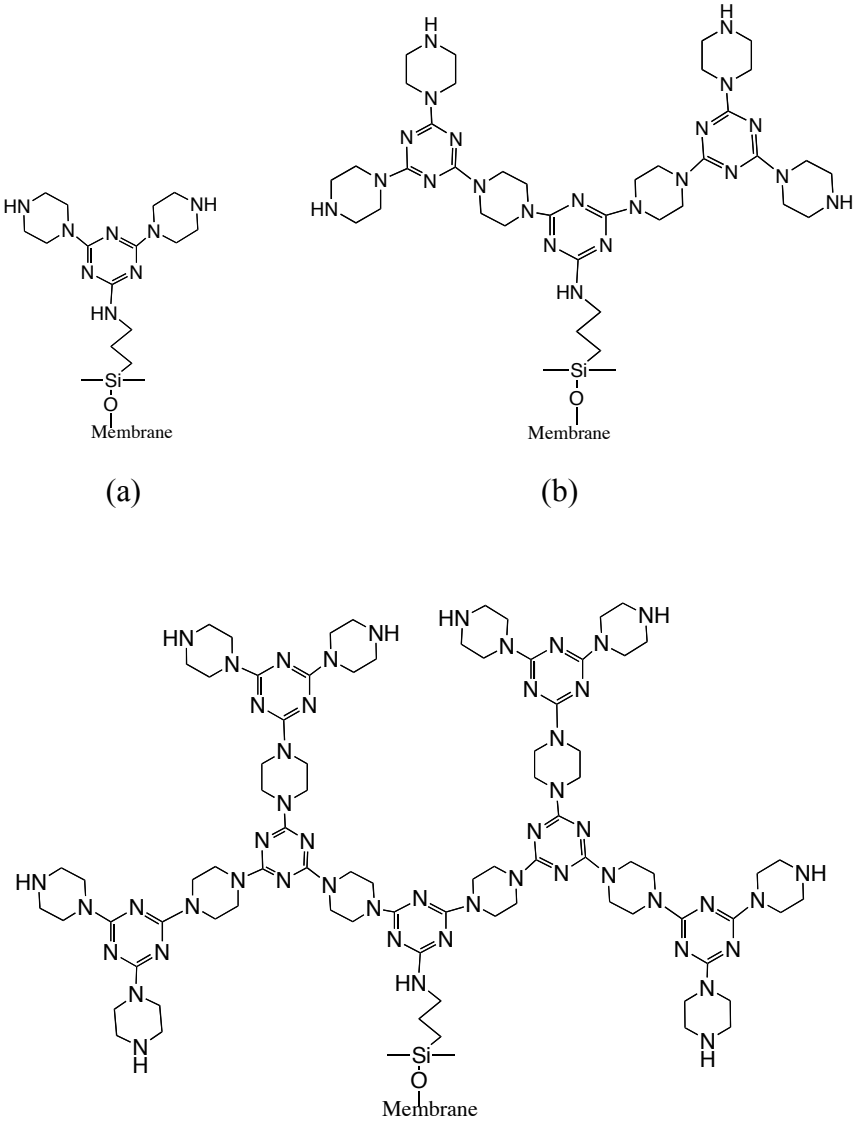

(a) (b)

(c)

Figure 8. G1- (a), G2- (b) and G3- (c) dendrons.

2.1.3 Dendrimer Architecture

In this work the primary diamine linkers used were, piperazine (PIP), 4-aminomethylpiperdine (AMP), p-xylylenediamine (XDA) and 4-aminobenzylamine (pABA). The capping groups used to terminate the dendrons were piperazine (PIP), allylamine, 4-aminobenzylamine (pABA), 4-aminomethylpiperidine (AMP) and p-xylylenediamine (XDA). Table 3 lists some of the samples investigated.

Table 3: Different linking groups and capping groups.

Dendrimer ID	Linking group	Capping group
G7-PIP	PIP	PIP
G3-Allylamine	PIP	Allylamine
G4-pABA	pABA	pABA
G4-AMP	AMP	AMP
G4-XDA	XDA	XDA

2.2 Synthesis of Cu(I)-Dendrimer Hybrid Membrane

In order to facilitate the transport of olefins, Cu(I) was introduced into the structure of dendrimers. Cu(I) wet-impregnation was also studied on ceramic membranes in various stabilizing solvents such as toluene, propionitrile and propylamine, which have been reported previously.

2.2.1 Materials

Cu(I)Br (purity,99.8%) was purchased from Aldrich. Diethylamine, propylamine, propionitrile and diethylenetriamine were purchased from Aldrich. Toluene and methanol were purchased from BDH. All chemical were used as received.

2.2.2 Preparation of Cu(I)-dendrimer Membrane

The idea of Cu(I)-dendrimer membrane was inspired by the strong complexing reaction between Cu(I)Br and amine groups. A dendrimer-functionalized membrane was added to a solution of 0.513 g Cu(I)Br (100 folds excess based on Cu(I)/amine 1:2 ratio) dissolved in 50 ml THF/methanol solvent. The entire reaction was performed on the Schlenk line, with continuous nitrogen purging at ambient temperature for 4 h. Then the membrane was washed with soxhlet extraction by THF, methanol, DCM and THF sequentially, 4 h for each solvent. The treated membrane was vacuum dried at 100 ˚C overnight and stored in a vial for measurement. Figure 9 shows schematically the synthesis concept.

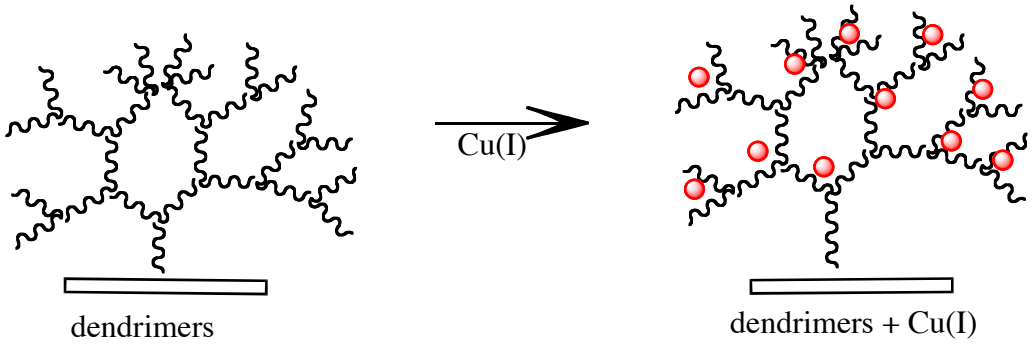

Figure 9. General experimental scheme of Cu(I)-dendrons.

2.2.3 Cu(I) Wet Impregnation (RCA Treated Membrane)

Cu(I) Diethylamine/diethylenetriamine Methanol System

In addition to the Cu(I)-dendrimer samples various combinations of Cu(I)Br and stabilizing ligands were studied to find the optimal solution when impregnated in RCA cleaned membranes without dendrimers. The diethylenetriamine/methanol system is described here as an example. The RCA treated membrane was added to a solution with 0.46 g diethylenetriamine dissolved in 50 ml methanol. The entire reaction was performed on the Schlenk line, with continuous nitrogen purging at ambient temperature for 4 h. The treated membrane was vacuum dried at 100 ˚C overnight and stored in a vial until testing.

Cu(I) Propionitrile/propylamine /toluene Systems

A RCA treated membrane was added into a 100 ml three-necked flask equipped with nitrogen gas inlet, Cu(I)Br powder (0.64 g) was dissolved in 50 ml toluene. Vigorous stirring and nitrogen purging were maintained to avoid the dissolving of oxygen and oxidation of Cu(I)Br. The reaction was performed at ambient temperature for 4 h and then the membrane was vacuumed dried at 100˚C overnight and stored in a vial for measurement. Also, propionitrile/propylamine systems were also carried out with the same procedure repeated. Table 4 shows the composition for each reaction.

Table 4. Reactant composition.

	Reactant Composition
I	0.64g Cu(I)Br+ 50 ml toluene
II	0.64g Cu(I)Br +0.46g diethylenetriamine + 50ml methanol
III	0.64g Cu(I)Br + 0.326 g diethylamine+ 50ml methanol
IV	0.64g Cu(I)Br + 50ml polylamine
V	0.64g Cu(I)Br + 50ml propaneitrile

2.3 Single Gas Permeation Test

Permeance measurements were carried out in a custom-built gas rig. Ultra high purity (99%) helium (He), nitrogen (N_2), carbon dioxide (CO_2), methane (CH_4), ethane

(C_2H_6), propane (C_3H_8), ethylene (C_2H_4) and propylene (C_3H_6) were purchased from AOC. Figure 10 shows the gas rig setup for single-gas measurement. The membrane was held in a shell-tube module and O-rings were used for proper sealing. The whole setup was connected to Labview, which records the mass flow rate, integral mass flow, and feed stream and permeate stream pressures. Users can set either the desired pressure and allow the control program to modulate mass flow according or vice versa.

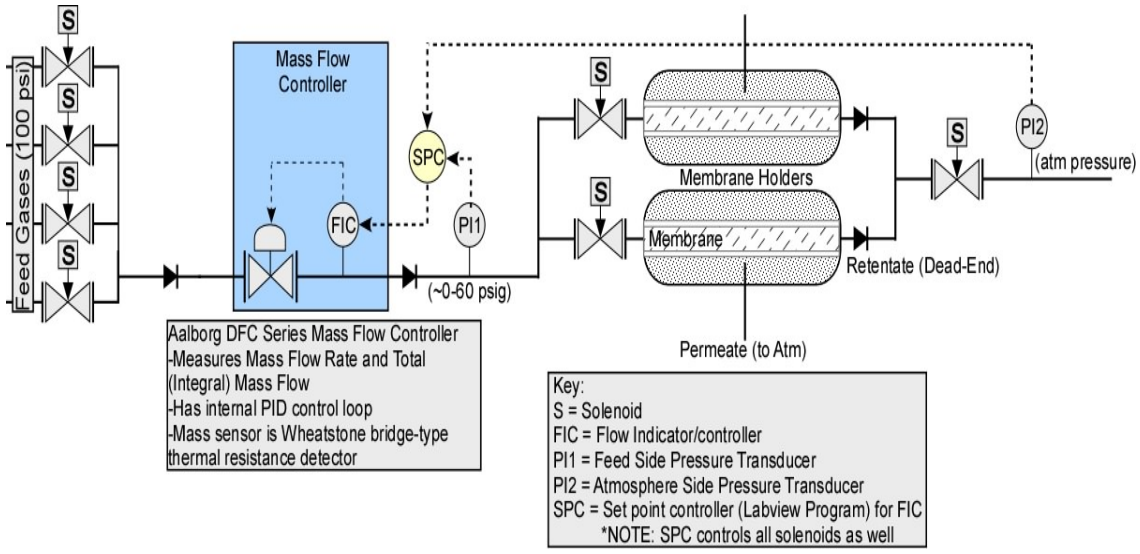

Figure 10. Schematic of custom-built permeance measurement gas-rig.

We noticed that permeances typically required some time to reach steady state for gases. It usually took longer for dendrimer membranes with lower permeance. For example, G3-based often require around 150s to get to steady state, while 1000s for G4-based membranes. Since the exact thickness of active layer is hard to measure for Membralox® membranes, the permeance was used to calculate the selectivity instead of permeability. The gas permeance was calculated from the volumetric flow rate. Eqn 2-1, 2-2, 2-3 show the permeance calculation:

$$N(mol/\sec) = Q \cdot (\frac{ml \cdot [STP]}{\min}) \times \frac{1l}{1000ml} \times \frac{1mol}{22.4l} \times \frac{1\min}{60\sec} \tag{2-1}$$

$$J(\frac{mol}{\sec \cdot m^2}) = \frac{N(mol/\sec)}{Area(m^2)} \tag{2-2}$$

$$P(\frac{mol}{\sec \cdot m^2 \cdot bar}) = \frac{J(mol/\sec \cdot m^2)}{\Delta p(bar)} \tag{2-3}$$

where Q is the volumetric flow rate, N is the mole flow rate, the area A is 0.000559 m^2 for Membralox® cylinder membrane, J is the gas flux, P is the permeance, and Δp is the pressure drop across the membrane.

CHAPTER III

REVERSE SELECTIVE MEMBRANES FORMED BY DENDRIMERS ON MESOPOROUS CERAMIC SUPPORTS

3.1 Introduction

This chapter summarizes the work on dendrimer-based hybrid membranes of light gas separations.

3.2 Experiment

Generation 1-7 dendrimers were synthesized on ceramic Membralox® membranes, as described in chapter II. Permeance measurements were performed with custom-built gas rig described in chapter II. Nitrogen (N_2), helium (He), carbon dioxide (CO_2), methane (CH_4), ethane (C_2H_6), propane (C_3H_8), ethylene (C_2H_4) and propylene (C_3H_6) (99.9 % purity) were tested. Unless noted, permeances were measured with a feed pressure of 24.3 psi.

3.3 Results

3.3.1 RCA Treated Membrane

Helium is a good indicator of membrane pinhole defects because it is the smallest gas molecule and surface diffusion can be safely ignored. Figure 11 shows the He permeance versus feed pressure. The results show that helium permeance is slightly dependent on the pressure range from 1.67 to 3.5 bar. A helium permeance independent of pressure indicates very low defect densities and that Knudsen transport dominates gas flow. Thus, Figure 11 indicates that for this membrane pinhole defects do not dominate the observed permeance.

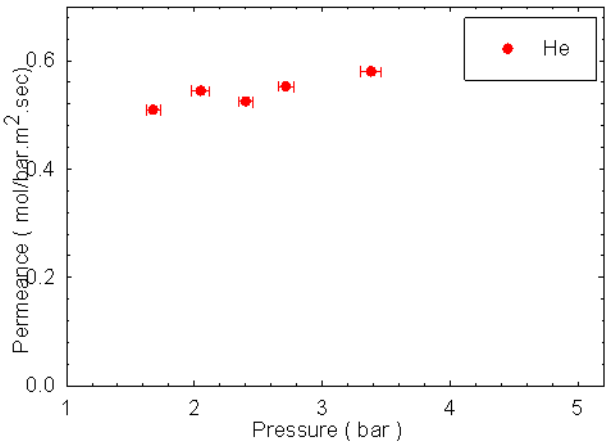

Figure 11. He permeance as a function of pressure for a RCA treated membrane.

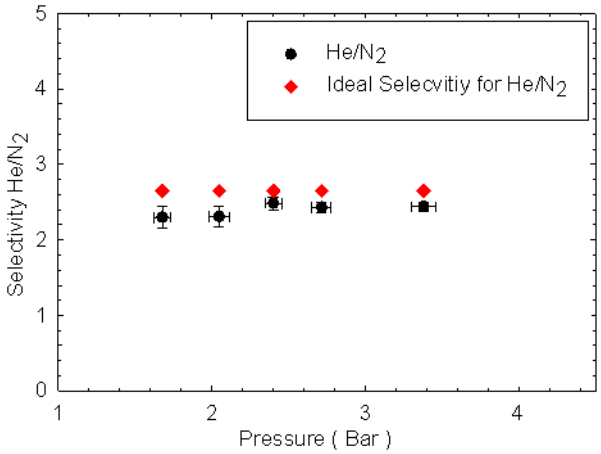

Figure 12. He/N_2 selectivity as a function of pressure of RCA treated membrane.

If Knudsen transport dominates the gas flow, the He/N_2 selectivity should be 2.65. Figure 12 shows that typical He/N_2 selectivity falls in the range of 2.2-2.5, slightly less than 2.65, which is consistent with previous literature indicating that these membranes tends to have a small numbers of pinhole defects [54]. Also nitrogen is known to weakly interact with hydroxyl groups on inorganic surfaces that can increase the surface flow through the ceramic supports [55], which causes the He/N_2 selectivity to be smaller than 2.65. These two factors both contribute to the reduction of the He/N_2 selectivity, although pinhole defects dominate separation ability.

3.3.2 Membrane with PIP Dendrons

Figure 13 shows the permeance performance for G1-PIP to G7-PIP functionalized membranes. The data clearly shows a significant decrease of permeances from G1-PIP to G7-PIP as anticipated. However, from generation one to generation five, the decrease is relatively small. In contrast, there is a dramatic transition point from generation five to generation six. The permeances of G6-PIP are almost 25 times lower than those of G5-PIP, which is a good indication of effective pore filling. Comparing the permeances of G6-PIP and G7-PIP, there is no obvious decrease of permeance. One interpretation of this is that the pores fill upon G6 formation and that it is impossible to effectively form G7. Another factor to be taken into consideration is the reaction yield for each generation. With the growth of dendrimer size, yields between dicholorotriazine and linking groups tend to decrease.

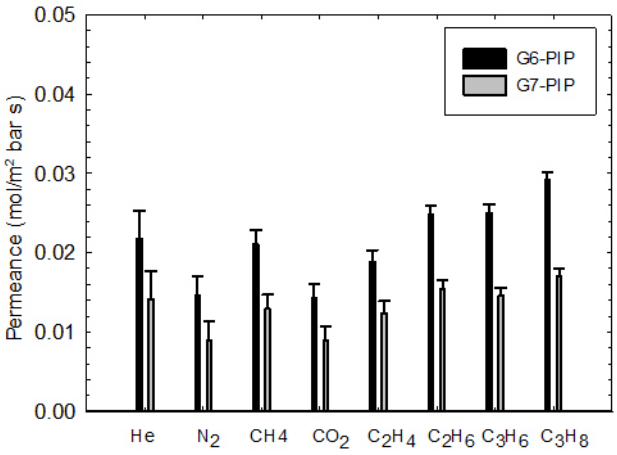

(a)

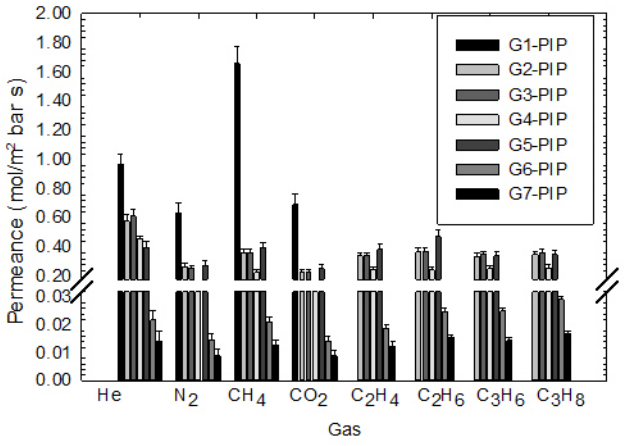

(b)

Figure 13. Permeance for G1-PIP to G7-PIP (G6-PIP and G7-PIP @ 80 psi).

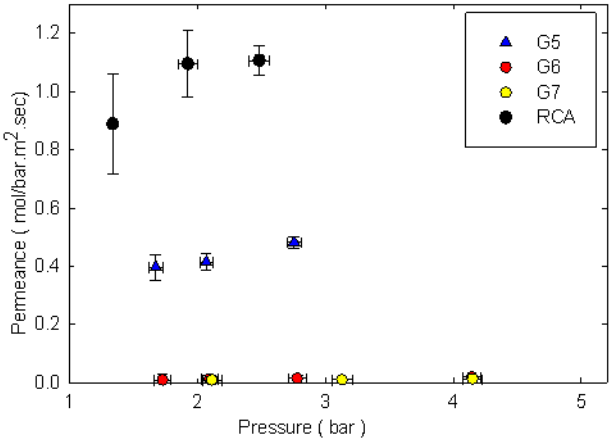

Figure 14. He permeance of G5-PIP, G6-PIP, G7-PIP and RCA treated membrane.

Figure 14 shows that permeance decreases from RCA treated membrane to G5-PIP, G6-PIP and then G7-PIP. However, from the helium permeance-pressure dependency plot, the slope of G5-PIP is smaller than that of RCA treated membrane. This could be interpreted as supportive evidence for filling the pores. To view this from another point, solubility-based separations can be analyzed by comparing the permeances of helium and propane. Freeman and Pinnau pointed out that [56] the goal of solubility separations is to remove small amounts of heavier/larger hydrocarbons from a light gas or mixture of light gases. In this case, when the solubility factor favors the transport process, it starts to show some benefits in C_3H_8/He separation. In other words,

the diffusivity ratio for the heavier gas/ lighter gas is always less than one. The free volume of the dendrimers tend to drive the diffusivity ratio to be close to unity and the solubility selectivity must be largely greater than one to offset the decrease in diffusivity selectivity [56]. Thus the C_3H_8/He selectivity can be viewed as an effective metric of pore sizes due to the small molecule size of helium and relatively condensable propane gas. Figure 15(a) gives the C_3H_8/He selectivity as a function of generation. The data in this plot shows that for G6-PIP and G7-PIP, C_3H_8/He selectivity is 1.2 and 1.33, which are greater than one. However, the ideal selectivity is 0.3 in the Knudsen region. These results indicate the Membralox®5nm pores have been fully filled with dendrimers. Figure 15 (b) shows the He/N_2 Robeson plot [57], while Figure 15 (c) shows the corresponding selectivity in the PIP-based membrane. Our G7-PIP membrane is showing an overall permeance performance up compared to previous reported permeance results, which locates at the right edge of Robeson plot. Though the selectivity is much lower than the reported data, the permeance is almost 10^4 higher than synthetic membranes. The aim here is to moderately increase selectivity while keeping such high permeances to benefit industrial separations, thus, the next step should be focused on the performance of selectivity.

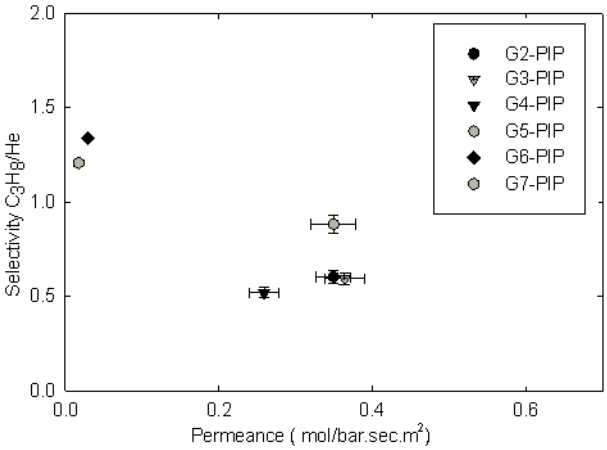

(a)

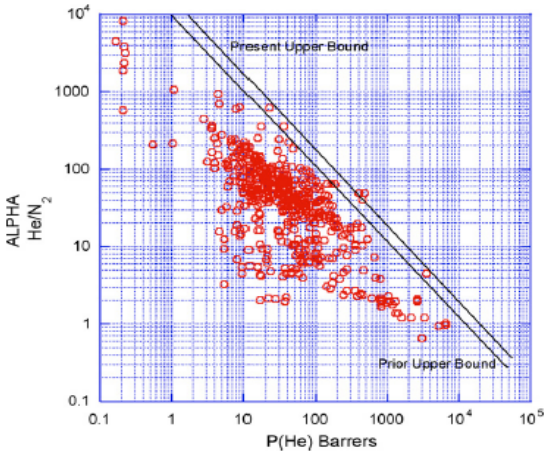

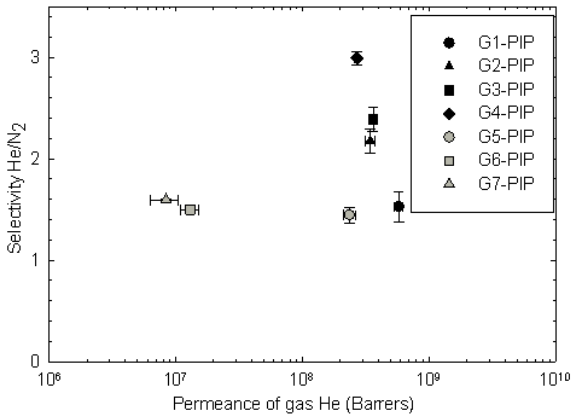

(b) (c)

Figure 15. CH_8/He selectivity for each generation (a), Robeson's He/N_2 correlation of separation factor versus permeability for polymeric membrane (b), He/N_2 correlation from G1-PIP to G7-PIP (c).

Figure 16 shows the separation performances of this composite membrane in the form of selectivity versus permeance. Most of the gas selectivities are identical to their ideal selectivities, even for G7-PIP. One possible reason is that the organic phase inside the pores is capable to reduce the flux. Another determining factor is that the solubility is not large enough to offset the unfavorable diffusivity. Thus, there is no significant enhancement in selectivity. For example, it has been reported that in the propane-methane separation, the solubility selectivity is always 10 times higher than most other materials, and diffusivity selectivity is always less than 1, which reasonably explains that the selectivity of C_3H_8/CH_4 is always greater than 1 [58,59]. One strategy can be employed to address this goal: increase the free volume of dendrimer structure. Further experiments should be designed to measure solubility and diffusivity quantitatively, which will lead to a better understanding of how to design high selectivity membranes.

However, promising selectivities for olefin/paraffin gases are not observed due to their similar solubilities and molecular size. A certain chemical facilitating agent needs to be introduced to selectively increase the olefin permeance.

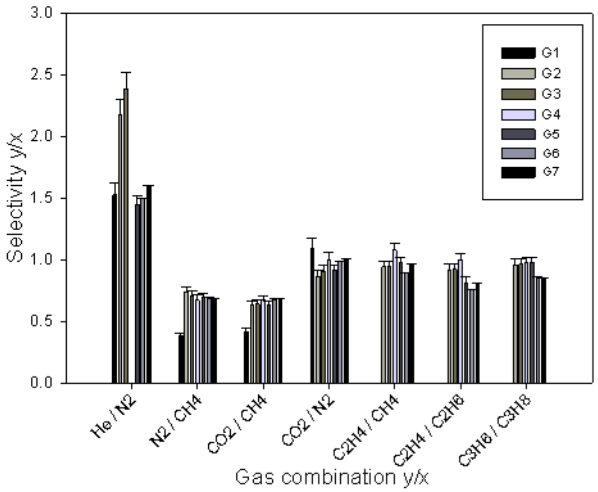

Figure 16. Selectivity for PIP-based dendrimer membrane.

3.3.3 Membrane with XDA Dendrons

Xylyldiamine was also used as a diamine spacer in the dendrimers. Utilizing different diamine linkers was explored to understand what effect the backbone chemistry has on gas permeance properties. [60].

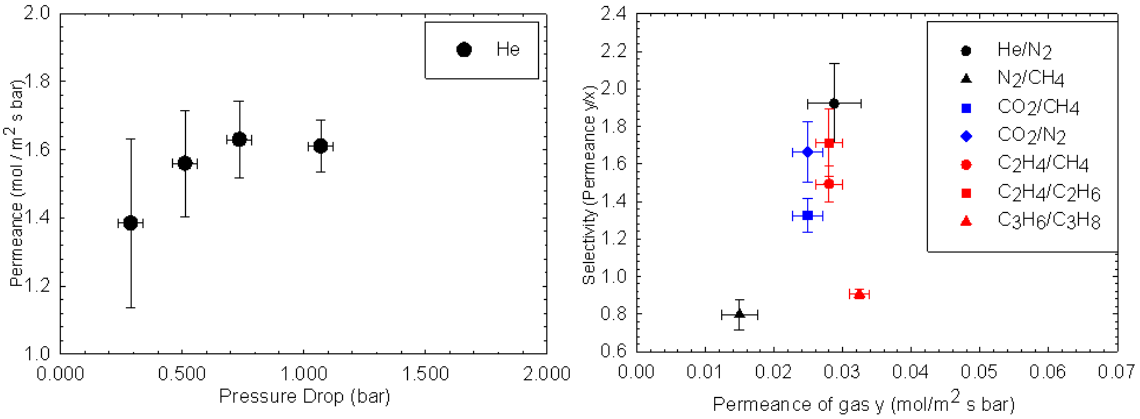

(a) (b)

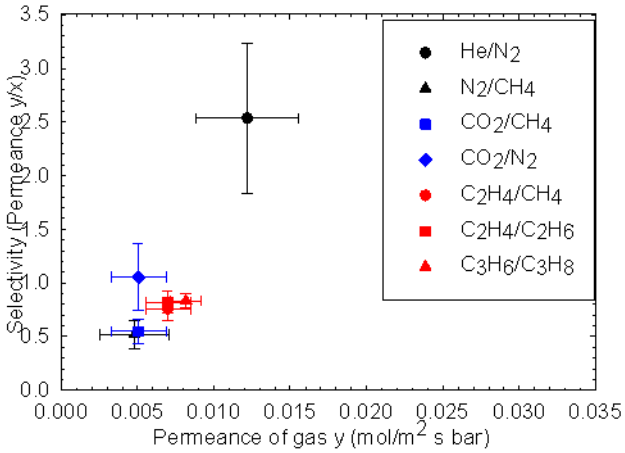

(c)

Figure 17. Selectivity as a function of permeance for RCA membrane (a) G2-XDA at 80 psi (b) and G3-XDA at 80 psi (c).

Figure 17 shows the permeances comparison for RCA membrane, G2-XDA and G3-XDA membranes. The permeances for G2-XDA are relatively low, on the magnitude of 10^{-2}, while most of the permeances for G3 membranes are in the region of 10^{-1} mol/bar.m^2.sec. G2-XDA also started to exhibit distinct time lag that we can observe. Since Daynes modeled the mass transport through a rubbery membrane and obtained a series of time lag data as a function of diffusion coefficient, this technique is employed in permeance measurement of porous membrane and polymer membrane [61]. The solubility and diffusivity coefficient can be determined from this model based on the solubility-diffusion and time lag model in the future.

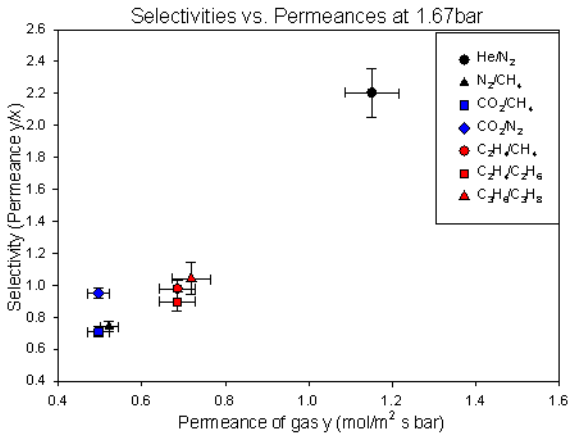

Figure 18. Selectivity as a function of permeance for G3-pABA membrane.

Figure 18 shows the selectivity as a function of permeance for the G3-pABA membrane. Distinguishable permeance differences between XDA and pABA membranes can be explained by the variety of amine group reactivities and molecular size. Originally, polymer crosslinking in gas separations was employed to prevent melamine plasticization. The crosslinking is likely to occur for linking groups with bifunctional amines, such as ethylenediamine, p-xylylenediamine, diethylenetriamine and polyethyleneimine [62].

Figure 19 shows the permeance comparison between G3-XDA and G4-XDA membranes. The permeances of G4-XDA for helium and nitrogen are similar to those of G3-XDA, but larger errors are observed. The flow rate of the G4-XDA membrane was near the lower limit for the gas rig, which makes it difficult to accurately measure gas permeances. The permeance greatly decreases from RCA to G2-XDA, however, a smaller permeance reduction is observed from G2-XDA to G4-XDA. There are three assumptions for XDA-dendrimer membrane. First, partially sites of XDA dendrimer might tend to crosslink and the remained reactive sites for cyanuric chloride becomes less, which leads to a small permeance reduction from G2-XDA to G4-XDA. More study will be performed in the future. Second, XDA dendrons, given they are larger than some of the other dendrons investigated, will fill the pores more quickly. Third, we believe that the XDA dendrons are glassier than other dendrons, and that they do not

collapse during thermal treatment. In contrast we believe that the dendrons with aliphatic amines are less likely to be globular upon high temperature drying. This would potentially explain the permeance performance for G7-PIP membrane.

The similarity between G4-XDA and G7-PIP permeances strongly suggest the plugging of the pores and the permeances both fall in the range of 10^{-3} mol/bar.m^2.bar. If diffusivity is the only factor taken into consideration, the comparable permeances between C_3H_8 and He can both be viewed as evidence of diffusion effects. However, since organic phase dendrimers in the pores will adsorb or dissolve a certain amount of gas, solubility factor also has to be considered. Time-lag measurements should provide information about these two influences. They will be performed in future work.

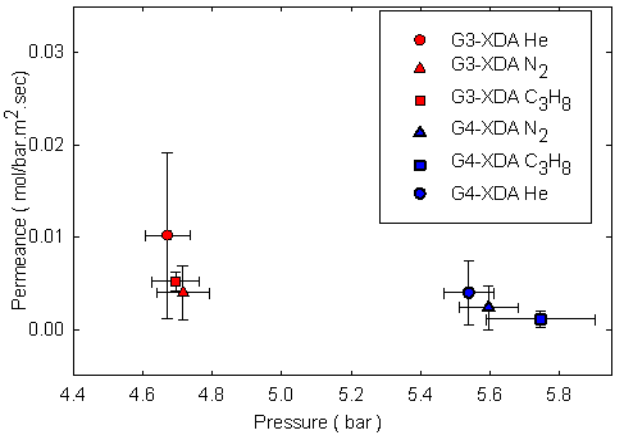

Figure 19. G3-XDA and G4-XDA pemeance as a function of pressure.

3.3.4 Membrane with Allylamine Dendrons

Dendrons were capped with allyl groups to introduce an olefin-based functionality. This architecture provides a large number of olefinic groups, which is expected to help improve olefin selectivity in olefin/paraffin separations. Figure 20 represents the permeance and selectivity for G3-Allylamine. The results show most of the gas permeances fall in the range from 0.3 – 0.5 mol/m^2.sec.bar. The selectivity for He/N_2 is approximately 2.3, which is slightly slower than the Knudsen ideal selectivity.

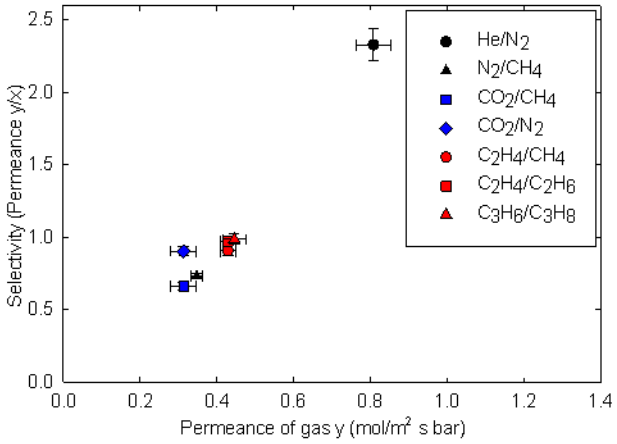

Figure 20. Selectivity as a function of permeance for G3-Allylamine.

3.3.5 Membrane with AMP dendrons

AMP has been chosen as a linking group due to its high reactivity. Figure 21 shows representative gas permeances for G3-AMP and G4-AMP. The permeances of G4-AMP were measured at 80 psi feed pressure due to the low permeances. The assumption could be made that the pores are almost filled for the G4-AMP membrane based on its permeance.

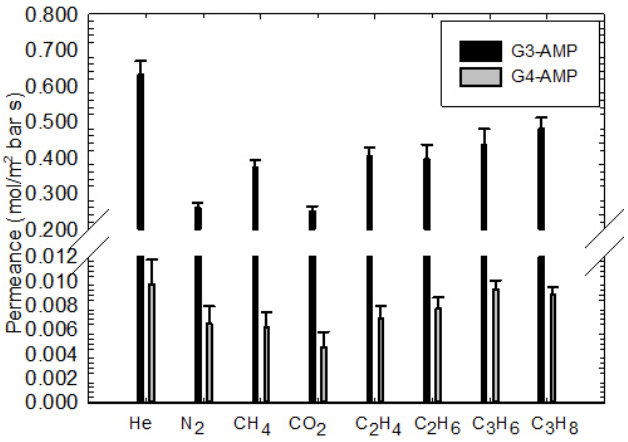

Figure 21. Permeance comparison between G3-AMP and G4-AMP membranes.

Figure 21 shows that He/N_2 selectivity drops from 2.42 to 1.49, which is also a good indicator that pores are becoming filled with organic. Figure 22 shows permeance

results for G3-AMP and G4-AMP. As He is the least affected gas by either physical adsorption or chemical interaction, the decrease of the He/N_2 selectivity is reasonably explained by the reduction of pore size for G4-AMP. However, he G4-AMP membrane has a slight selectivity of C_2H_4/CH_4 approximately 1.2.

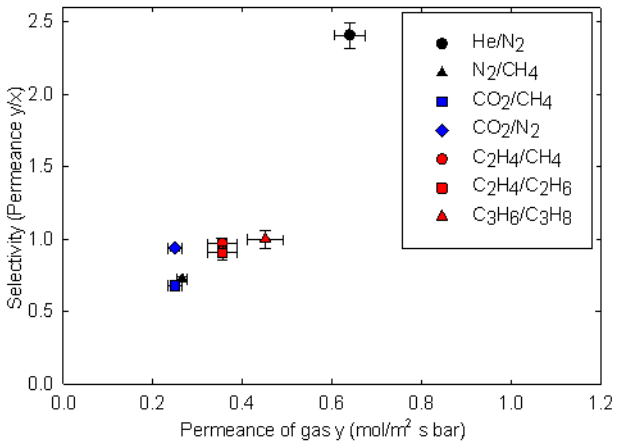

(a)

Figure 22. Selectivity versus permeance for G3-AMP (a) and G4-AMP (b).

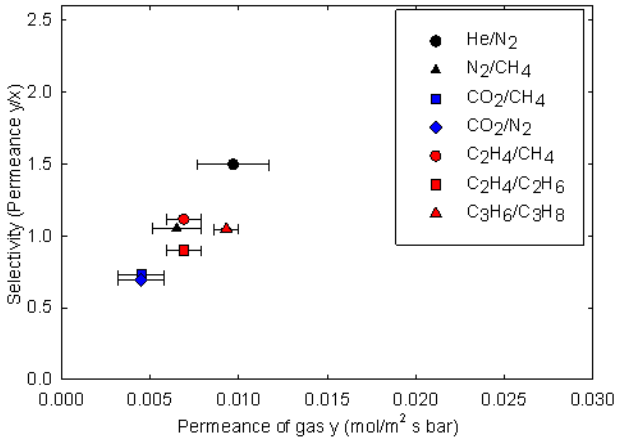

(b)

Figure 22. Continued.

Comparing G3-based dendrimer data with previous work it is clear that the permeances are almost 100 times higher. Several reasons could explain this. The first is the robust drying procedure, which removes most of the solvent inside or outside the pores.. The second is the RCA treatment procedure, which enlarges the pores and makes generation three dendrimer inefficiently fill the pores. The third reason is the dendrimer possibly collapsing after high temperature treatment for allylamine, PIP and AMP-based membrane, which will reduce the pore size as well. However, the XDA-based membranes are likely to maintain their permeance even after high temperature thermal treatment. More research needs to be done to support this hypothesis, such as permeance

testing before and after solvent treatment. Assuming collapsing occurs after vacuum drying, the permeance should goes down after solvent treatment because the dendrimer starts to relax its conformation.

Table 4 compares the permeances for a variety of dendrimer membranes based on this work. The membranes exhibit distinct performances due to the different physical and chemical properties of linking groups. It can be seen that G7-PIP, G4-AMP and G3-XDA reach comparable permeances.

Table 4. The effect of dendrimer generation on permeance.

Dendrimer	**Generation and permeance (magnitude) comparison**						
PIP	**G1**	**G2**	**G3**	**G4**	**G5**	**G6**	**G7**
	10^{-1}	10^{-1}	10^{-1}	10^{-1}	10^{-1}	10^{-2}	10^{-3}
Allylamine	**G1**	**G2**	**G3**				
	10^{-1}	10^{-1}	10^{-1}				
AMP	**G1**	**G2**	**G3**	**G4**			
	10^{-1}	10^{-1}	10^{-1}	10^{-3}			
XDA	**G1**	**G2**	**G3**	G4			
	10^{-1}	10^{-2}	10^{-3}	10^{-3}			

3.4 Conclusions

We have made a variety of dendrimer-base hybrid membranes by synthesizing G7-PIP, G4-AMP, G3-Allylamine and G3-XDA. The permeances are relatively high due to robust drying procedure and RCA treatment. The results clearly demonstrate that the pores are not filled for most of third generation membranes. However, for AMP, PIP, XDA-utilized membranes, higher generation is capable to effective fill the pores based on the increasing of C_3H_8/He selectivity.

CHAPTER IV

Cu(I)-BASED FACILITATED MEMBRANES FOR OLEFIN/PARAFFIN SEPARATIONS

4.1 Introduction

Olefin/paraffin separations play important role in the petrochemical industry, as they are important feedstocks for polymer production [63]. Conventional separations such as distillation are energy intensive since the olefin and paraffin boiling points are very similar. Chapter III showed the separation and permeance performance of dendrimer-based hybrid membranes. An alternate approach is to use facilitated transport membranes (FTM) [64]. The motivation for the next step is to design Cu(I)-attached membranes specified for olefin and paraffin separations. This chapter has three components: 1) the development of Cu(I) uptake on dendrimer functionalized membranes; 2) wet impregnation of Cu(I) onto RCA treated membranes; 3) design optimal metal-chelating system to stabilize Cu(I) and facilitate olefin transport.

4.2 Experiment

A variety of chelating groups, such as diethylenetriamine, diethylamine and solvent, such as methanol, propylamine, propionitrile have been employed to synthesize facilitated transport membranes with the procedure described in Chapter II. These compounds are shown in Figure 23.

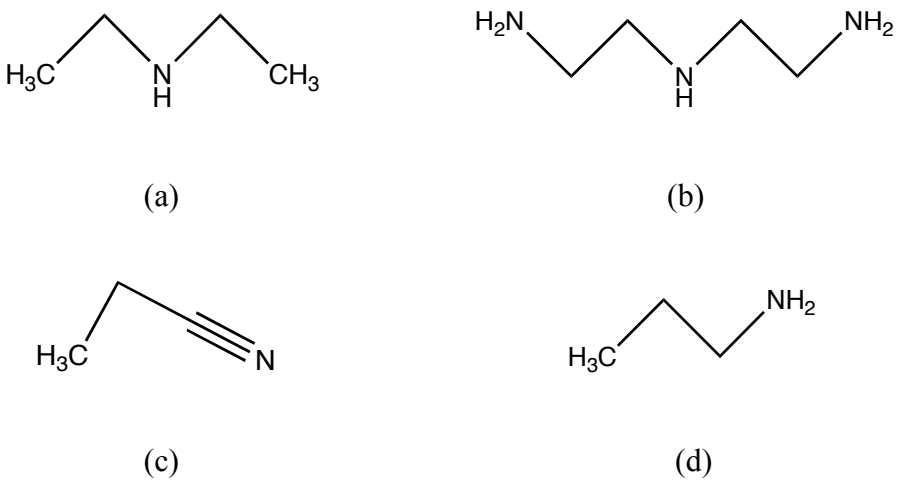

Figure 23. Chemical structure of chelating groups, diethylamine (a), diethylenetriamine (b), propionitrile (c), propylamine (d).

4.3 Results

4.3.1 Cu(I)-AMP Dendrimer Hybrid Membrane

The main focus was on Cu(I)-AMP-functionalized dendrimer membranes. To assess the reproducibility of Cu(I) functionalization, three parallel experiments were designed. They were adding two distinctive G3-AMP membrane pieces and one G4-AMP membrane piece into a Cu(I) solution.

Figure 24 shows the selectivity versus permeance for the G3-AMP-Cu(I) membranes. G3-AMP-Cu(I) #1 and #2 were synthesized with the same procedures. The C_2H_4/CH_4 selectivities are 0.96 and 1.40 for the membrane pieces, while the C_3H_6/C_3H_8 selectivities are 1.62 and 1.01 for the corresponding membrane piece, respectively. Moreover, a certain number of factors should be taken into consideration in studying the selectivity-permeance relationship. One possible reason could be oxidation of Cu(I). In aqueous systems, the cupric state of copper is more stable than the cuprous state [65]. Eqn 4-1 shows the occurrence of Cu(I) disproportionation in aqueous solution.

$$2Cu(I) \underset{K_1}{\rightarrow} Cu^0 + Cu(II) \tag{4-1}$$

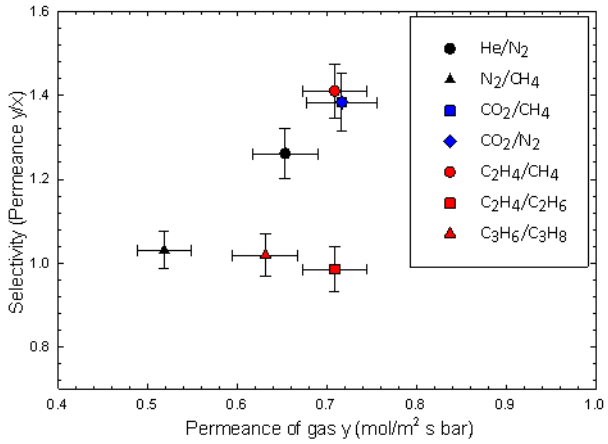

(a)

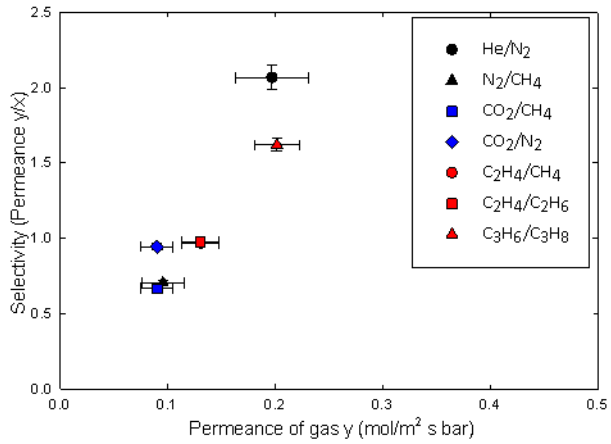

(b)

Figure 24. Selectivity versus permeance for G3-AMP-Cu(I) #1(a), G3-AMP-Cu(I) #2 (b).

Thus, an oxygen free environment must be maintained and moisture must be strictly avoided during the reaction [66]. A trace amount of oxygen dissolved in solvent could result in great differences in chelating with Cu(I). After oxidation, Cu(II) will easily coordinate with some hard bases, such as water. Vallee and Williams [67] showed that Cu(II) tends to favor six-coordinate octahedral geometries, but Cu(I) tends to exhibit four-coordinate tetrahedral geometries. There is always a competition between Cu(I), Cu(II), solvent and olefin, which can be described as the Eqn 4-2, 4-3, 4-4, 4-5, 4-6:

$$2Cu(I) \underset{K_1}{\leftrightarrow} Cu^0 + Cu(II) \tag{4-2}$$

$$Cu(II) + aL \underset{K_2}{\leftrightarrow} Cu(II)L_a \tag{4-3}$$

$$Cu(I) + bL \underset{K_3}{\leftrightarrow} Cu(I)L_b \tag{4-4}$$

$$Cu(I) + dOL \underset{K_4}{\leftrightarrow} Cu(I)(OL)_d \tag{4-5}$$

$$Cu(I)L_b + dOL \underset{K_4}{\leftrightarrow} Cu(I)L_b(OL)_d \tag{4-6}$$

where L represents the stabilizing ligand or solvent and OL represents an olefin ligand.

These points suggest how permeance influences the binding capacity between Cu(I) and olefins such as ethylene and propylene. Also, the permeance of He effectively

reflects the characteristic pore size after Cu(I) impregnation. For example, permeance of He for G3-AMP#1 is 0.97 mol/bar.m^2.sec, which is larger than that of G3-AMP#2, 0.63 mol/bar.m^2.sec. If assuming the same amount of Cu(I) was attached onto the membrane, for larger olefin molecules such as propylene are likely to complex with Cu(I), which results in the increase of selectivity of gas pair propylene/propane, rather than ethylene/methane.

There have been efforts to model facilitated transport membranes (FTM). The acceptable mechanism of FTM can be described as two steps: a diffusion controlling step (fast reaction), and a reaction controlling step (slow reaction). Bessarabov shows that the separation of ethylene/ethane using silver nitrate as facilitating agent, almost no facilitation is observed at low carrier concentration. And facilitation occurs till a certain critical loading [68]. Therefore, the concentration of Cu(I) plays an important role in order to increase the selectivity of olefins/paraffins.

Fig 25 shows the relation between selectivity and permeance for the G4-AMP-Cu(I) membrane. The C_2H_4/CH_4 and C_3H_6/C_3H_8 selectivities went back to near Knudsen selectivity (0.73 and 0.76, respectively). Several reasons can be predicted to address this point. First, an appropriate concentration of Cu(I) has to be reached and if the Cu(I) concentration is too low, the complexation reaction can not take effect. Second, an appropriate solvent needs to be chosen. If the solvent binding capacity is too strong and

it will form a stable complex with Cu(I), it is hard to remove the solvent even at high temperature and will decrease Cu(I)-olefin binding affinity. Third, diffusivity is still to be strongly considered in the separation process. Even if there is enough Cu(I) on the membrane surface to make complexation happen, small molecules can still pass through the membrane very easily due to the relatively large pore size. Fourth, amine interaction with Cu(I) severely reduced the olefin complexing capacity.

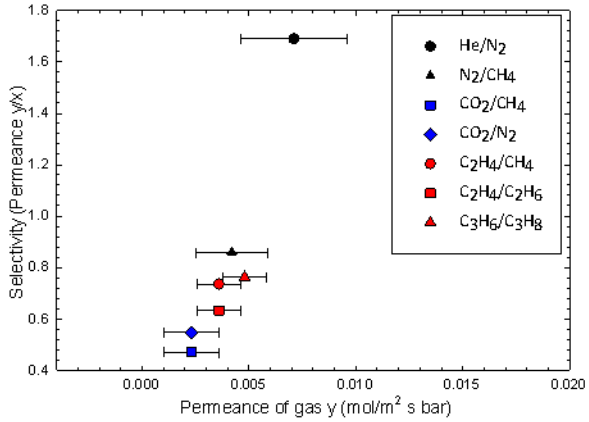

Figure 25. Selectivity versus permeance for G4-AMP-Cu(I) membrane.

4.3.2 Cu(I) Wet Impregnation of RCA Treated Membrane

The likely occurrence of Cu(I)-olefin complexation is determined by the following factors : nature of solvent, nature of stabilizer and the concentration of Cu(I). The whole process can be described in Figure 26. From the previous results for Cu(I)-dendrimer membranes, the following experiments have been carried out to give general ideas about how Cu(I) concentration influences the permeance of the membrane. Figure 26 is a schematic of the Cu(I) wet impregnation processes: first, a Cu(I) layer is deposited on the alumina surface based on the interaction between Cu(I) and hydroxyl groups. Next, multiple Cu(I) layers are uniformly distributed on the first layer. The solvent is removed from the alumina surface by thermal treatment. In this way, RCA treated membrane is expected to be fully occupied by Cu(I) ions in order to facilitate olefin transport.

Figure 27 shows that C_2H_4/CH_4 selectivity stays the same with RCA treated membrane, which is slightly higher than Knudsen selectivity. After one Cu(I) impregnation the C_3H_6/C_3H_8 selectivity increased to 1.43 due to the appropriate Cu(I)-olefin complexing. Figure 28 (a) shows the C_3H_6 permeances change as a function of impregnation cycle. The hypothesis could be made that after one/two impregnations of Cu(I), the membrane surface is almost saturated with Cu(I) ion.

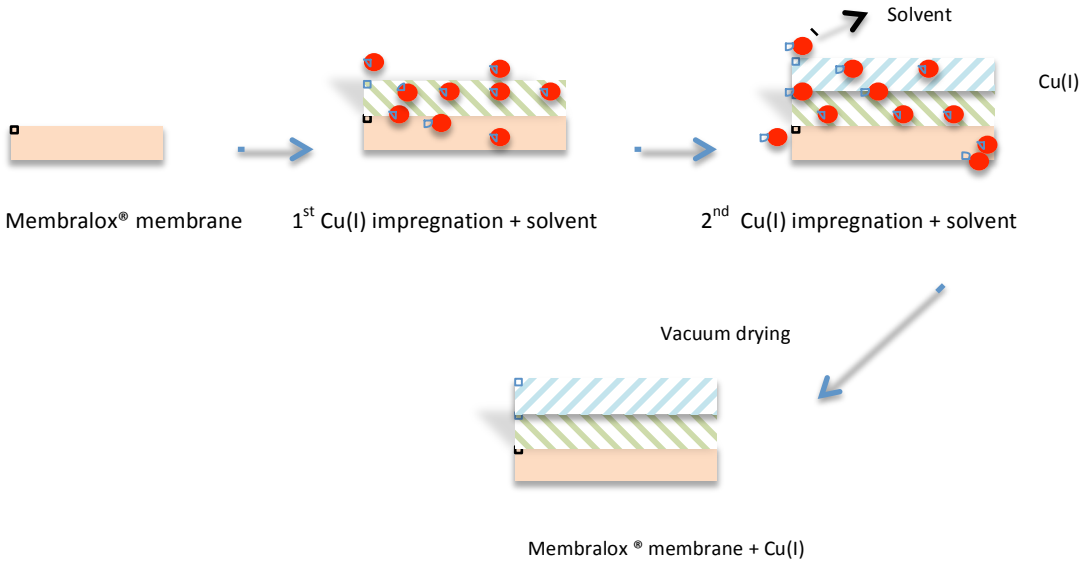

Figure 26. Multiple Cu(I)-impregnation synthetic protocols.

To our knowledge, no report has been published about the long-time stability of composite membranes containing Cu(I) salts. However, one of the most characteristic properties of ion is the ionic mobility. Each ion will be stabilized can be further stabilized by forming a chelating bond [69]. The wet impregnation of Cu(I) can be assumed by the process of forming layers. Thus, after the first/second layer on the ceramic support, the ability to add more layers tends to decrease. The results for the one Cu(I) impregnation shows contrary trends with those we have discussed before. The most likely fact is the occurrence of weak complexing between Cu(I) and propylene

which facilitated the transport of olefin through membrane. However, further research needs to be done to explore the diffusivity and facilitator factor in this experiment.

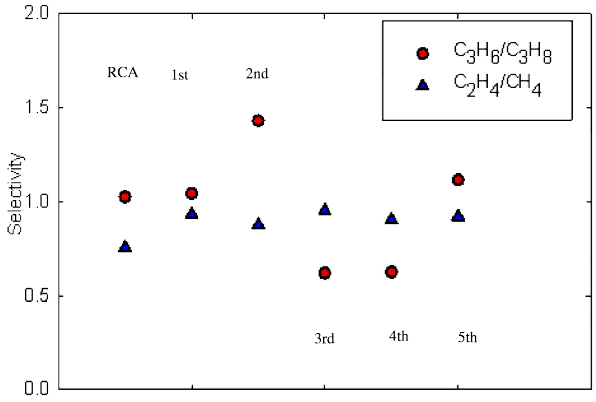

Figure 27. C_3H_6/C_3H_8, C_2H_4/CH_4 selectivity, from left to right represent ideal selectivity, RCA treated membranes, one-, two-, three- and four-time coating with Cu(I), respectively.

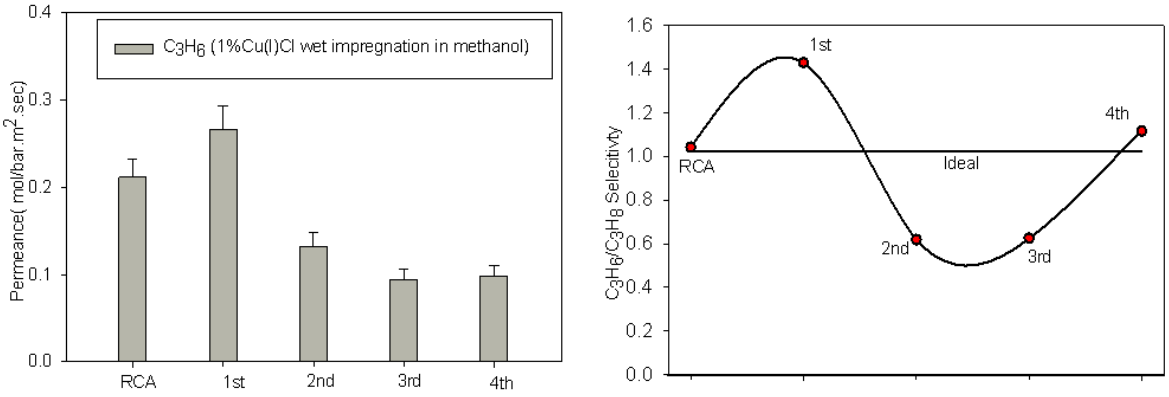

(a) **(b)**

Figure 28. Propylene permeance change as a function of Cu(I) impregnation cycle (a) C_3H_6/C_3H_8 selectivity change as a function of Cu(I) impregnation cycle (b).

4.3.3 Cu(I)-stabilizing Ligand-solvent Systems

Based on previous information about multiple-impregnations of Cu(I), there is a slight increase of olefin/paraffin selectivity after one impregnation. But the instability is still the key in the wet impregnation technique. Therefore, various Cu(I)-stabilizing ligand-solvent systems have been studied to facilitate the transport of olefin and stabilize Cu(I) from disproportionation. The goal was to maintain Cu(I) in the monovalent state r by complexing with the proper solvent, which has relatively weaker competition with the olefin [65].

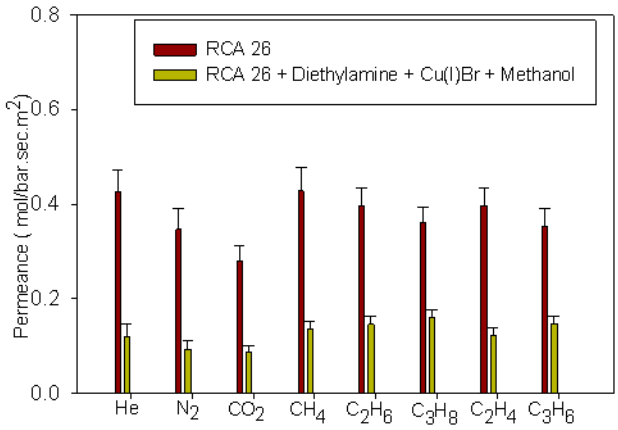

Figure 29. Permeances for RCA treated membrane before and after Cu(I)-diethylamine-methanol treatment.

Figure 29 shows representative data for the Cu(I)-diethylamine-methanol system. The data shows a significant decrease of permeance after the membrane is treated with Cu(I) and diethylamine, which is approximately 0.08 mol/bar.m^2.sec. However, some differences are observed for various systems. Figure 30 explains the N_2 permeances reducing with stabilizing ligands, such as diethylamine, diethylenetriamine, propionitrile, propylamine and toluene.

First, the solubility trend for Cu(I) in the threes solvents were toluene (almost insoluble)< methanol (0.4%, solubility based on weight per 100g solvent) < propylamine (16%-18%) < propionitrile (40%) [65]. The solubility factor reasonably explains that the

permeance decreases only by 30% for toluene because of the low solubility of Cu(I) in toluene. Though there was some evidence showing that toluene was the least effective in terms of olefin complexing capacity [65], it was difficult to carry out because the concentration of Cu(I) in solvents still dominates the process of Cu(I) wet impregnation. For the systems with diethylenetriamine, diethylamine, propionitrile and propylamine, N_2 permeances reduced by 70% - 95% on the basis of RCA treated membranes. These results strengthen the prediction we made from the results of Cu(I)-dendrimer membranes before that amine interaction with Cu(I) severely reduces the olefin complexing capacity. However, Cu(I)-propionitrile systems showed the largest reduction in N_2 permeance. The high solubility of Cu(I) in propionitrile and moderate capacity of stabilizing Cu(I) in its monovalent state contributed to the high-loading of Cu(I), which is preferred for this research.

Samples were also made using wet impregnation of Cu(I)-propionitrile systems. The Cu(I)-propionitrile membrane has similar permeance properties between G3-AMP and G4-AMP membrane. The boiling point of propionitrile is 97.2 ˚C and so the thermal treatment was increased to 120˚C in order to dry and completely remove the solvent. Figure 31 shows the selectivity after depositing Cu(I) on RCA treated membranes from propionitrile solutions.

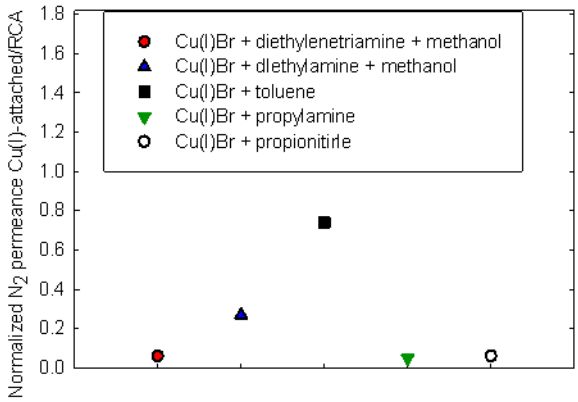

Figure 30. Reduction of N_2 permeance after Cu(I) added into various systems.

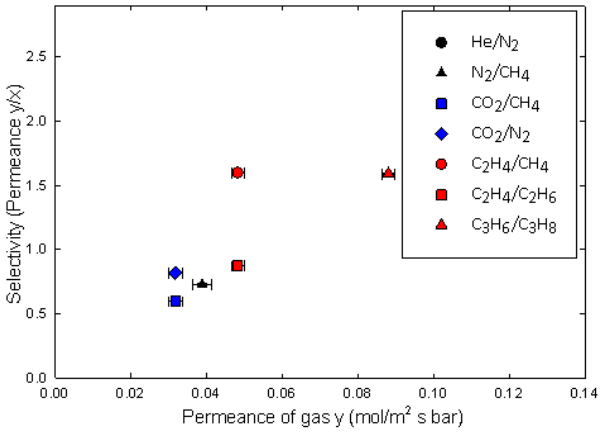

Figure 31. Selectivity for Cu(I)-propionitrile membrane (120˚C).

The use of priopionitrile/Cu(I) solutoins affected olefin/paraffin selectivity, which could be explained by the higher solubility of Cu(I) in propionitrile. Blytas [65] pointed out that competition between olefin and solvent for Cu(I) decreases in the order of propylamine > propionitrile > toluene. In turn, complexing lowers the ability of Cu(I) binding with olefins and increase their solubilities. Andrew [70] performed studies on electron rich N-donor ligands, which were incorporated into Cu(I)-olefin interaction. He found out copper atoms in each complex tend to coordinate to two pyridine nitrogen atoms and appropriate number of olefins. Further studies need to be done to explore the interaction between nitriles and olefins.

4.4 Conclusions

In this chapter, wet impregnation of Cu(I) has been studied on RCA treated membranes. The mobility of Cu(I), stabilizing ligands, solvents were observed to affect the permeances of RCA membrane, then the capacity to facilitate olefin/paraffin separations. Cu(I)/propionitrile system has been proved to be the optimal solvent/stabilizing ligand for facilitated transport membranes. Further research is still needed to study the application of this system to the dendrimer-based membranes.

CHAPTER V

FUTURE WORK AND CONCLUSIONS

5.1 Synthesis of Uniform Mesoporous Silica Membralox®

One area for future work is preparing defect-free alumina substrate due to the industrial fabrication limitation since a small amount of pinhole defects will strongly affect the performance. Thus, a uniform mesoporous substrate is desired to achieve high permeane and selectivity performance. Also, a certain number of membranes with pinhole defects are found based on the previous study, which can be theoretically predicted from He/N_2 selectivity and permeance-pressure dependency plot of helium. Two main techniques are mainly used to address this point, simple dip-coating or inside dip-coating. A solution that contains solvent ethanol, silica precursor Brij 56, surfactant TEOS and HCl was prepared to perform deposition on the ceramic membrane. The problem of removing surfactant and solvent is critical in the coating process, which can be achieved by high temperature calcination and solvent extraction. However, there are some limitations for these two methods. Calcination causes pore shrinkage and collapse, whereas solvent extraction does not completely remove the surfactant. Figure 32 illustrates the preparations for defect-free membranes. The whole process can be viewed

as layer-by-layer deposition technique. Thus, small defects or cracks can usually be repaired by repeating dip-coating cycles. Also, the roughness of substrate surface greatly determines the permeation performance. The flux is high because coating thickness can be minimized on the polished substrate [71].

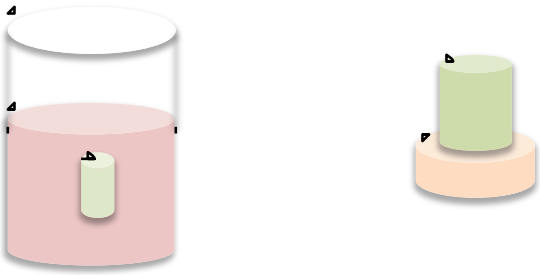

(a) **(b)**

Figure 32. Synthesis methods for defect-free membrane: (a) simple dip-coating, and (b) inside dip-coating.

Dependence on pressure drop for helium and large He/N_2 deviations from Knudsen ideal selectivity will provide strong evidence that defects or cracks are present with the membrane. The best way to check this is to test the gas permeance before and after dip-coating procedure. Smaller dependency or independency should be observed if the dip-coating method is effective.

5.2 ATRP-based Hybrid Membrane

A large variety of methods have been developed to functionalize membrane surface to change charge density, surface roughness and porosity, address specific membrane separation applications. A controlled mechanism, surface-initiated atom transfer radical polymerization (ATRP) has been increasingly chosen to achieve this modification. Compared with the dendrimer chemistry, described in Chapter II, there are some benefits for this approach: 1) short time are required for the whole reaction processes, compare to dendrimer chemistry; 2) ATRP technique is very easy and robust; 3) effective thickness of grafted polymers on the membrane walls can be predicted from the gas permeance data; 4) ARTP chemistry is flexible by altering the choice of the monomer; 5) can from " polymer-brush" structures on the membrane surface [72-75]. Based on the previous related work [76] in our lab, ATRP is an effective technique to be introduced into membranes. Figure 33 shows the synthetic protocols for ATRP-functionalized mesoporous alumina membrane.

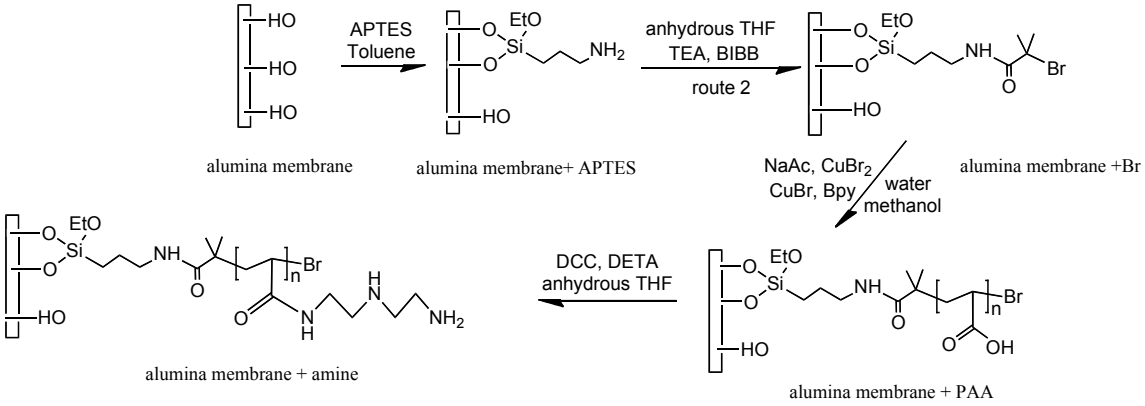

Figure 33. Synthetic protocols for ATRP functionalized mesoporous alumina membrane [76].

5.3 Cu(I)-propionitrile System

The great potential of olefin/paraffin separation of Cu(I)-propionitrile has been observed and will be further studied. The amount of Cu(I) loading on the membrane and its thermal treatment will be the crucial for separation factor based on previous work. A series of experiment with varying Cu(I)-concentration solutions will be performed to explain how Cu(I) loading influences the olefin/paraffin separation factor. Another factor to be taken into consideration is the thermal treatment of Cu(I)-propionitrile membrane. An additional set of experiments with multiple temperature values will be carried out to illustrate the effects of thermal treatment.

REFERENCES

[1] W.S. Winston, K.K. Sirkar, Membrane Handbook, Van Nostrand Reinhold, New York, 1992.

[2] M. Mulder, Basic Principle of Membrane Technology, Kluwer Academic Publishers, Dordrecht, 1996.

[3] M.C. Porter, Handbook of Industrial Membrane Technology, Noyes Publication, New Jersey, 1990.

[4] R.W. Baker, Membrane Technology and applications, John Wiley & Sons Ltd, England, 2004.

[5] M. Cheryan, Ultrafiltration and Microfiltration handbook, CRC Press, Florida, 1998.

[6] M. Panar, R.R. Hebert, The nature of asymmetry in reverse osmosis membranes, Macromolecules 6 (1973) 777-780.

[7] B.D. Freeman, Membrane gas separation, Wiley, United Kingdom, 2010.

[8] K. Scott, Handbook of Industrial Membranes, Elsevier Advanced Technology, UK, 2006.

[9] K. Keizer, R.J.R. Uhlhorn, Membrane Separation Technology, Principles and Applications, Amsterdam: Elsevier, 1995.

[10] H. Choi, E. Stathatos, D.D. Dionysiou, Sol–gel preparation of mesoporous photocatalytic TiO_2 films and TiO_2/Al_2O_3 composite membranes for environmental applications, Applied Catalysis B: Environment 63 (2006) 60-67.

[11] M. Cheryan, Ultrafiltration and Microfiltration, CRC Press, Florida, 1998.

[12] L.M. Robeson, Correlation of separation factor versus permeability for polymeric membranes, Journal of Membrane Science 62 (1991) 165-185.

[13] B.D. Freeman, Basis of Permeability/Selectivity tradeoff relations in polymeric gas separation membranes, Macromolecules 32 (1999) 375-380.

[14] M. Ulbricht, Advanced functional polymer membranes, Polymer 47 (2006) 2217-2262.

[15] P.E. Odendall, Water Treatment Membrane Processes, AWWA Research Foundation, US, 1996.

[16] S.J. Yoo, D.M. Ford, D.F. Shantz, Synthesis and characterization of uniform alumina-mesoporous silica hybrid membrane, Langmuir 22 (2006) 1839-1845.

[17] A. Javaid, D.M. Ford, Solubility-based gas separation with oligomer-modified inorganic membranes, Journal of Membrane Science 187 (2001) 141-150.

[18] T. Okui, Y. Saito, Gas permeation of porous organic/inorganic hybrid membranes, Journal of So-gel Science and Technology 5 (1995) 127-134.

[19] J.R. Miller, W.J. Koros, The formation of chemically modified γ-alumina microporous membranes, Separation Science and Technology 25 (1990) 1257-1280.

[20] J. Randon, P. Blanc, R. Paterson, Modification of ceramic membrane surfaces using phosphoric acid and alkyl phosphonic acid and its effects on the ultrafiltration of BSA protein, Journal of Membrane Science 98 (1995) 119-129.

[21] K.C. McCarley, J.D. Way, Development of a model surface flow membrane by modification of porous γ -alumina with octadecytrichlorosilane, Separation Purification Technology 25 (2001) 195-210.

[22] A. Javaid, E.E. Simanek, David M. Ford, Nanocomposite membranes of chemisorbed and physisorbed molecules on porous alumina for environmentally important separations, Journal of Membrane Science 275 (2006) 255-260.

[23] T.C. Merkel, B.D. Freeman, A.J. Hill, Ultrapermeable reverse-selective nanocomposite membranes, Science 296 (2002) 519-522.

[24] S.J Yoo, S. Yeu, D.F. Shantz, Reverse-selective membranes formed by dendrimers on mesoporous ceramic supports, Journal of Membrane Science 314 (2009) 16-22.

[25] S.J. Yoo, J.D. Lunn, D.F. Shantz, Engineering nanospaces: OMS/dendrimer hybrids possessing controllable chemistry and porosity, Chemistry of Materials 18 (2006) 2935-2942.

[26] Q.Q. Wang, D.F. Shantz, Catalytic properties of dendron-OMS hybrids, Journal of Catalysis 269 (2010) 15-25.

[27] S. Yeu, J.D. Lunn, D.F. Shantz, The effect of surface modifications on protein microfiltration properties of Anopore™ membranes, Journal of Membrane Science 327 (2009) 108-117.

[28] E.E. Simanek, The 8 year thicket of triazinedendrimers: strategies, targets and applications, Proceedings of the Royal Society A 466 (2010) 1445-1468.

[29] W. Zhang, S.O. Gonzalez, E.E. Simanek, Structure-Activity relationships in dendrimers based on triazines: gelation depends on choice of linking and surface groups, Macromolecules 35 (2002) 9015-9021.

[30] W. Zhang, E.E. Simanek, Dendrimers based on melamine. Divergent and orthogonal, convergent syntheses of a G3 dendrimer, Organic Letters 2 (2000) 843-845.

[31] W. Zhang, D.T. Nowlan, E.E. Simanek. Orthogonal, Convergent Syntheses of dendrimers based on melamine with One or Two unique Surface Sites for manipulation, Journal of the American Chemical Society 123 (2001) 8914-8922.

[32] H. Crampton, E.E. Simanek, A divergent route towards single-chemical entity triazine dendrimers with opportunities for structural diversity, New Journal of Chemistry 31 (2007) 1283-1290.

[33] J. Lim, E.E. Simanek, Toward the next-generation drug delivery vehicle: synthesis of a dendrimer with four orthogonally reactive groups, Molecular Pharmaceutics 2 (2005) 273-277.

[34] K.X. Morena, E.E. Simanek, Identification of diamine linkers with differing reactivity and their application in the synthesis of melamine dendrimers, Tetrahedron Letters 49 (2008) 1152-1154.

[35] R.B. Eldridge, Olefin/paraffin separation technology: A review, Industrial & Engineering Chemistry Research 32 (1993) 2208-2212.

[36] R.B. Eldridge, D.J. Safarik, Olefin/paraffin separations by reactive absorption: A review, Industrial & Engineering Chemistry Research 37 (1998) 2571-2581.

[37] W.S. Winston, Kamalesh K. Sirkar, Membrane Handbook, Van Nostrand Reinhold, New York, 1992.

[38] T. Rosenberg, The concept of carrier transport and its corollaries in pharmacology, Pharmocol Reviews 13 (1961) 109-183.

[39] R.D. Hughes, J.A. Mahoney. E.F. Steigelmann, Olefin separation by facilitated transport membranes, Recent Developments in Separation Science 173 (1986).

[40] I. Pinnau, L.G. Toy, Solid polymer electrolyte composite membranes for olefin/paraffin separation, Journal of Membrane Science 184 (2001) 39-48.

[41] M.T. Ravanchi, A. Kargari, Application of membrane process in petrochemical industry: a review, Desalination 235 (2009) 199-244.

[42] R.B. Eldridge, D.J. Safarik, Olefin/paraffin separations by reactive absorption: A review, Industrial & Engineering Chemistry Research 37 (1998) 2571-2581.

[43] A.F. Scott, B. Rubin, Preparation of copper (I) trifluoroacetate carbonyl Inorganic Chemistry 11 (1969) 2533-2534.

[44] W.J. Koros, R. Mahajan, Pushing the limits on possibilities for large scale gas separation: which strategies, Journal of Membrane Science 175 (2000) 181-196.

[45] P.G. Carman, Flow of gases through porous media, Academic Press Inc, New York, 1956.

[46] S.V. Sotirchos, V.N. Burganos, Transport of gases in porous membranes, MRS Bulletin 24 (1999) 41-45.

[47] W. Kern, D.A. Puotien, Cleaning solutions based on hydrogen peroxide for use in silicon semiconductor technology, RCA Rev 31 (1970) 187-206.

[48] J. Schultz, K.V. Peinemann, Membranes for separation of higher hydrocarbons from methane, Journal of Membrane Science 110 (1996) 37-45.

[49] N.N. Li, J.M. Calo, Separation and purification technology, Marcel Dekker Inc, New York, 1992.

[50] R.B. Eldridge, Olefin/Paraffin separation Technology: A review, Industrial & Engineering Chemistry Research 32 (1993) 2208-2212.

[51] J. Chen, R.B. Eldridge, A study of Cu(I)-ethylene Complexation for olefin-paraffin separation, AICHE Journal 57 (2001) 630-644.

[52] D. HR, J. Wu, Structurally characterized coinage-metal-ethylene complexes, European Journal of Inorganic Chemistry 4 (2008) 509-522.

[53] A. Javaid, D.M. Ford, Solubility-based gas separation with oligomer-modified inorganic membranes Part III. Effects of synthesis conditions, Journal of Membrane Science 246 (2005) 181-191.

[54] R.P. Singh, P. Jha, K. Kalpakci, J.D. Way, Dual-surface-modified reverse-selective membranes, Industrial & Engineering Chemistry Research 46 (2007) 7246-7252.

[55] K.C. McCarley, J. D. Way, Development of a model surface flow membrane by modification of porous γ-alumina with octadecyltriclorosilane, Separation and Purification Technology 25 (2001) 195-210.

[56] B. Freeman, I. Pinnau, Separation of gases using solubility-selective polymers, Trip 5 (1997) 167-173.

[57] L.M. Robeson, The upper bound revisited, Journal of Membrane Science 320 (2008) 390-400.

[58] K. Nagai, A. Higuchi, T. Nakagawa, Gas permeability and stability of poly(1-trimethylsilyl-1-propyne-co-1-phenyl-1-propyne) membranes, Journal of Polymer Science Part B: Polymer Physics 33 (1995) 289-298.

[59] I. Pinnau, C.G. Casillas, B.D. Freeman, Hydrocarbon/hydrogen mixed gas permeation in poly(1-trimethylsiyl-1-propyne) (PTMSP), poly(1-phenyl-1-propyne) (PPP), and PTMSP/PPP blends, Journal of Polymer Science Part B: Polymer physics 34 (1996) 2613-1621.

[60] M.B. Steffensen, E.E. Simanek, Dendrimers based on [1,3,5]-triazines, Journal of Polymer Science: Part A: Polymer Chemistry 44 (2006) 3412-3433.

[61] S.W. Rutherford, D.D. Do, Review of time lag permeation technique as a method for characterization of porous media and membranes, Adsorption 3 (1997) 283-312.

[62] K. Vanherck, A.C. Odena, I. Vankelecome, A simplified diamine crosslinking method for PI nanofiltration membranes, Journal of Membrane Science 353 (2010) 135-143.

[63] T.A. Reine, R.B. Eldridge, Absorption equilibrium and kinetics for ethylene-ethane separation with a novel solvent, Industrial & Engineering Chemistry Research 44 (2005) 7505-7510.

[64] R.W. Baker, Future directions of membrane gas separation technology, Industrial & Engineering Chemistry Research 41 (2002) 1391-1411.

[65] G.C. Blytas, Separation of unsaturates by complexing with nonaqueous solutions of cuprous salts. Separation and Purification Technology; Li,N.N; Marcel Dekker: New York, 1992; Chapter 2.

[66] S.J. Son, H.S. Kim, S.W. Kim, Selective absorption of isoprene from C_5 mixtures by π complexation with Cu(I), Industrial & Engineering Chemistry Research 44 (2005) 4717-4720.

[67] E.A. Ambundo, M.V. Deydier, D.B. Rorabacher, Influence of coordination geometry upon copper (II/I) redox potentials. Physical parameters for twelve copper tripodal ligand complexes, Inorganic Chemistry 38 (1999) 4233-4242.

[68] I. Pinnau, T.C. Merkel, Transport properties of PA12-PTMO/$AgBF_4$ solid polymer electrolyte membranes for olefin/paraffin separation, Desalination 145 (2002) 347-351.

[69] H. Sigel, R.B. Martin, Coordinating properties of the amide bond. Stability and structure of metal ion complexes of peptides and related ligands, Chemical Reviews 82 (1982) 385-426.

[70] J.J. Allen, A.R. Barron, Olefin coordination in copper(I) complexes of bis(2-pyridyl)amine, Dalton Transactions (2009) 878-890.

[71] B.A. McCool, J. DiCarlo, W.J. Desisto, Synthesis and characterization of mesoporous silica membranes via dip-coating and hydrothermal deposition techniques, Journal of Membrane Science 218 (2003) 555-67.

[72] A. Friebe, M. Ulbricht, Controlled pore functionalization of Poly(ethylene terephthalate) track-etched membranes via surface-initiated atom transfer radical polymerization, Langmuir 23 (2007) 10316-10322.

[73] F.J. Xu, J.P. Zhao, J. Li, Functionalization of nylon membranes via surface-initiated atom-transfer radical polymerization, Langmuir 23 (2007) 8585-8592.

[74] Z.P Cheng, X.L. Zhu, K.G. Neoh, Modification of poly(ether imide) membranes via surface-initiated atom transfer radical polymerization, Macromolecules 39 (2006) 1660-1663.

[75] N. Singh, S.M. Husson, Modification of regenerated cellulose ultrafiltration membranes by surface-initiated atom transfer radical polymerization, Journal of Membrane Science 311 (2008) 225-234.

[76] Y.H. Zhao, D.F. Shantz, Phenylboronic acid functionalized SBA-15 for sugar capture, Langmuir 27 (2011) 14554-14562.

VITA

Name:	Ting Liu
Address:	Texas A&M University, TAMU 3122, College Station, TX 77843
Email Address:	peggyzju@tamu.edu or zhudi.lt@gmail.com
Education:	B.S., Chemical Engineering, Zhejiang University, 2009 M.S., Chemical Engineering, Texas A&M University, 2012